ANL-6864
Reactor Technology
(TID-4500, 37th Ed.)
AEC Research and
Development Report

ARGONNE NATIONAL LABORATORY
9700 South Cass Avenue
Argonne, Illinois 60440

EBR-II WET CRITICAL EXPERIMENTS

by

F. S. Kirn
Idaho Division

and

W. B. Loewenstein
Reactor Physics Division

October 1964

Operated by The University of Chicago
under
Contract W-31-109-eng-38
with the
U. S. Atomic Energy Commission

DISCLAIMER

TABLE OF CONTENTS

LIST OF FIGURES

LIST OF TABLES

EBR-II WET CRITICAL EXPERIMENTS

by

F. S. Kirn and W. B. Loewenstein

I. INTRODUCTION

The Experimental Breeder Reactor-II (EBR-II) Wet Critical Experiments are one phase of a comprehensive, experimental, neutronic investigation associated with that reactor system. The Wet Critical Experiments are so designated to distinguish them from the previously conducted Dry Critical Experiments.[1] The Wet Critical Experiments were conducted with sodium coolant in the reactor system, while the similar low-power investigations comprising the Dry Critical Experiments were performed with essentially no sodium coolant in the reactor system. Other pertinent, low-power, neutronic investigations include the detailed engineering mockup of EBR-II on the Zero Power Reactor-III (ZPR-III),[2] as well as several related, but relatively clean, geometry systems that were also studied on ZPR-III.[2] The next EBR-II neutronic studies comprise the Approach to Power.* These studies will emphasize power-dependent and long-term irradiation neutronics, as well as a few low-power investigations. The low-power investigations include measurements relating to the conversion ratio of the system based on fission rate distribution in core and blanket.

The EBR-II Wet Critical Experiments were designed to provide two general, but not mutually exclusive, types of information. First there are the data that are essential for operating the power reactor system. These include control rod worth, neutron source strength, nuclear instrument response, etc. The second type of data is of more general interest, including the total worth of the sodium coolant, critical size, and the isothermal temperature coefficient of reactivity.

The most interesting implication of results from the Wet Critical Experiments comes from comparison with predicted parameters and measured results from both the Dry Critical Experiments and the EBR-II Mockup on ZPR-III. In general, extrapolations of the previous experimental data were in substantial agreement with the results reported here; they were also in good agreement with theory. The performance of all three types of critical experiments (e.g. Zero Power Mockup, Dry Critical Experiments, and Wet Critical Experiments), along with satisfactory extrapolations among the three, does suggest that some of the investigations may,

*The Approach to Power was initiated during July 1964.

in fact, have been partly repetitive. That this is the case could not have been ascertained with confidence before these experiments were performed. However, the general analytical improvements that have been developed[3] since this program was initiated, coupled with the EBR-II experience, may serve as a guide toward a judicious choice of experimental neutronics for future, fast reactor system investigations. In making such choices, one should not overlook the implications of zero-power experimental investigations on similar systems in clean geometry which were also extensively studied on ZPR-III.[2]

In addition to providing the neutronic data, the Wet Critical Experiments were the first opportunity to operate the reactor system in its normal situation. Most of the experiments were performed at 600°F, and thus the program provided considerable information pertaining to verification of engineering design. These aspects will not be considered in this report.

Finally, the Wet Critical Experiments may give some insight into the problems of translating neutronic specifications into an actual engineering system.

II. DESCRIPTION OF THE EBR-II

The EBR-II power plant complex (Fig. 1) is located at the United States Atomic Energy Commission National Reactor Testing Station and includes a complete, remotely-operated, fuel-processing and fuel-element fabrication facility. It is the first reactor in the United States Power Reactor Demonstration Program to operate on a closed fuel cycle. Partly spent or burned fuel is pyrometallurgically reprocessed, re-enriched, and returned to the reactor after being refabricated.

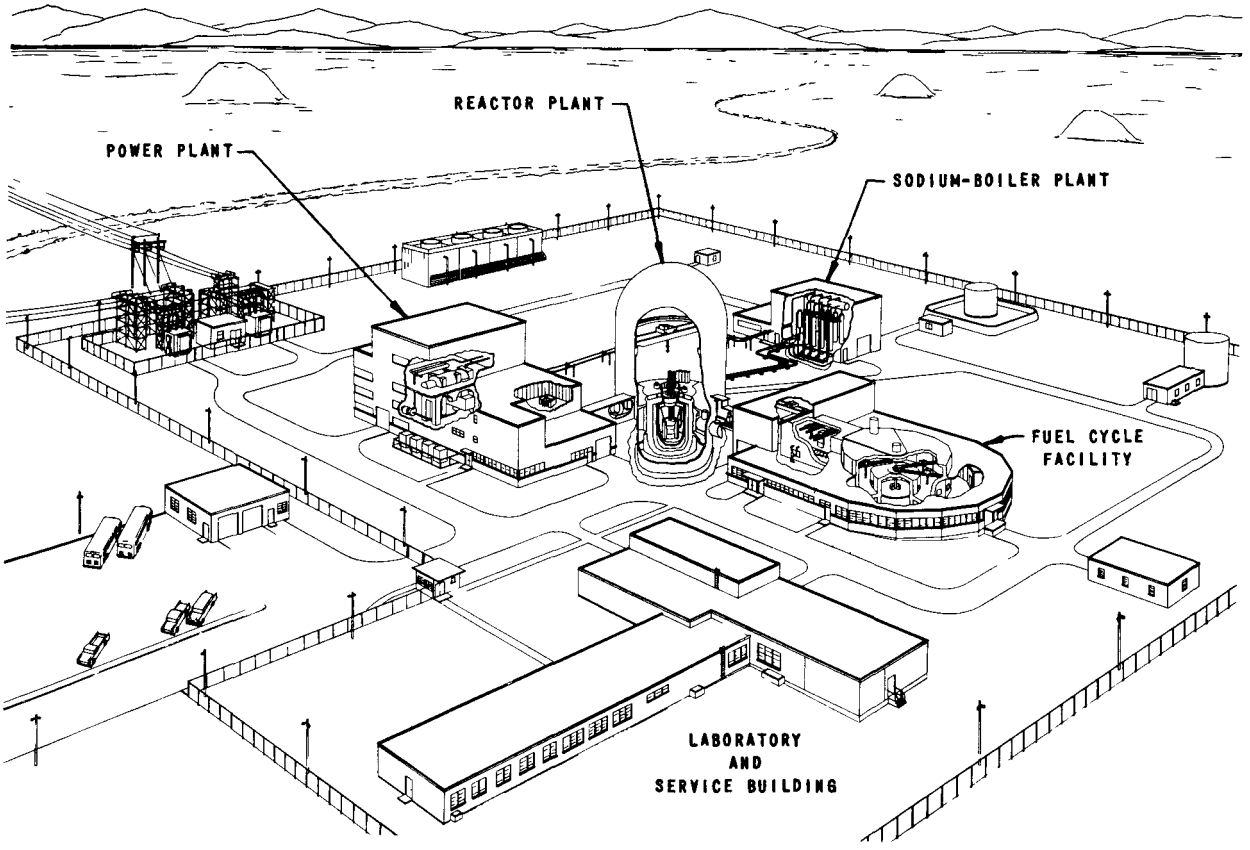

111-7032-A

Fig. 1. EBR-II Facility

The reactor is submerged in the primary tank (Fig. 2), containing about 90,000 gal of liquid sodium at 370°C. With a 9000-gpm maximum rate of coolant flow in the reactor, the large sodium reservoir ensures that temperature transients in the bulk coolant are slowly transmitted to the reactor. The large sodium reservoir also serves as a partial heat sink for shutdown cooling in case of failure of the primary cooling system. The primary tank is suspended inside an airtight containment building (Figs. 2 and 3) which is designed to confine an accidental release of fission products, plutonium, and activated sodium from the primary system.

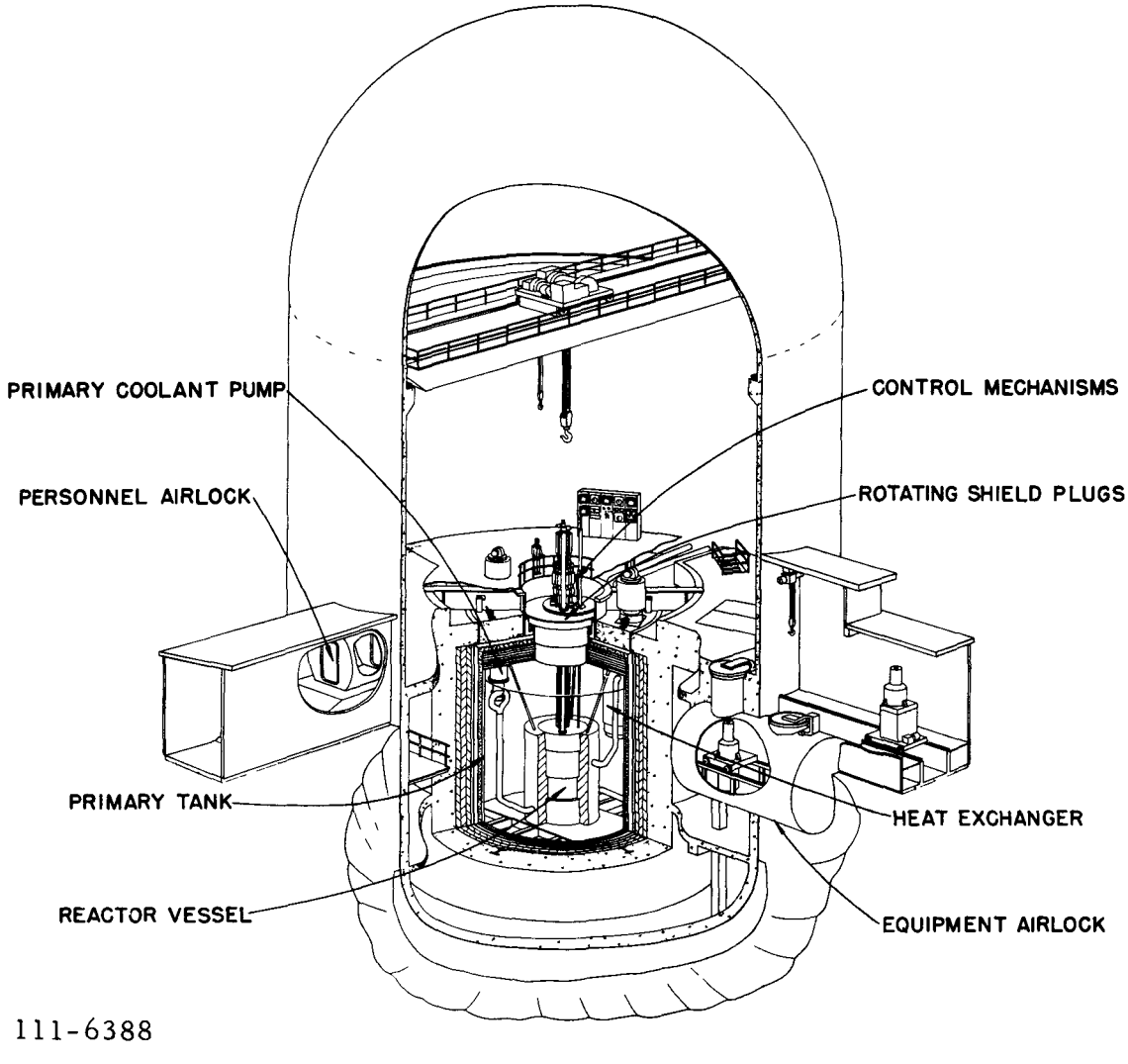

Fig. 2. EBR-II Reactor Plant

The reactor building is designed to confine the effects of a maximum sodium-air interaction caused by a major sodium release. In a sense, the reactor is thus doubly contained.

The reactor is in the reactor vessel near the bottom of the primary tank (Fig. 3). Coolant is taken from the bulk sodium in the primary tank, passed through two 5000-gpm mechanical pumps, and introduced near the bottom of the reactor vessel. Flow is then upward through individual fuel and breeder-reflector subassemblies. To achieve nearly uniform temperatures of the coolant at the outlet, the coolant flow is orificed in a manner consistent with axial and radial power-density gradients and discontinuities. The hot (482°C) coolant leaves the reactor near the top of the reactor vessel and then passes through the primary heat exchanger submerged in the primary sodium. Sodium is the working fluid of the intermediate, secondary cooling system.

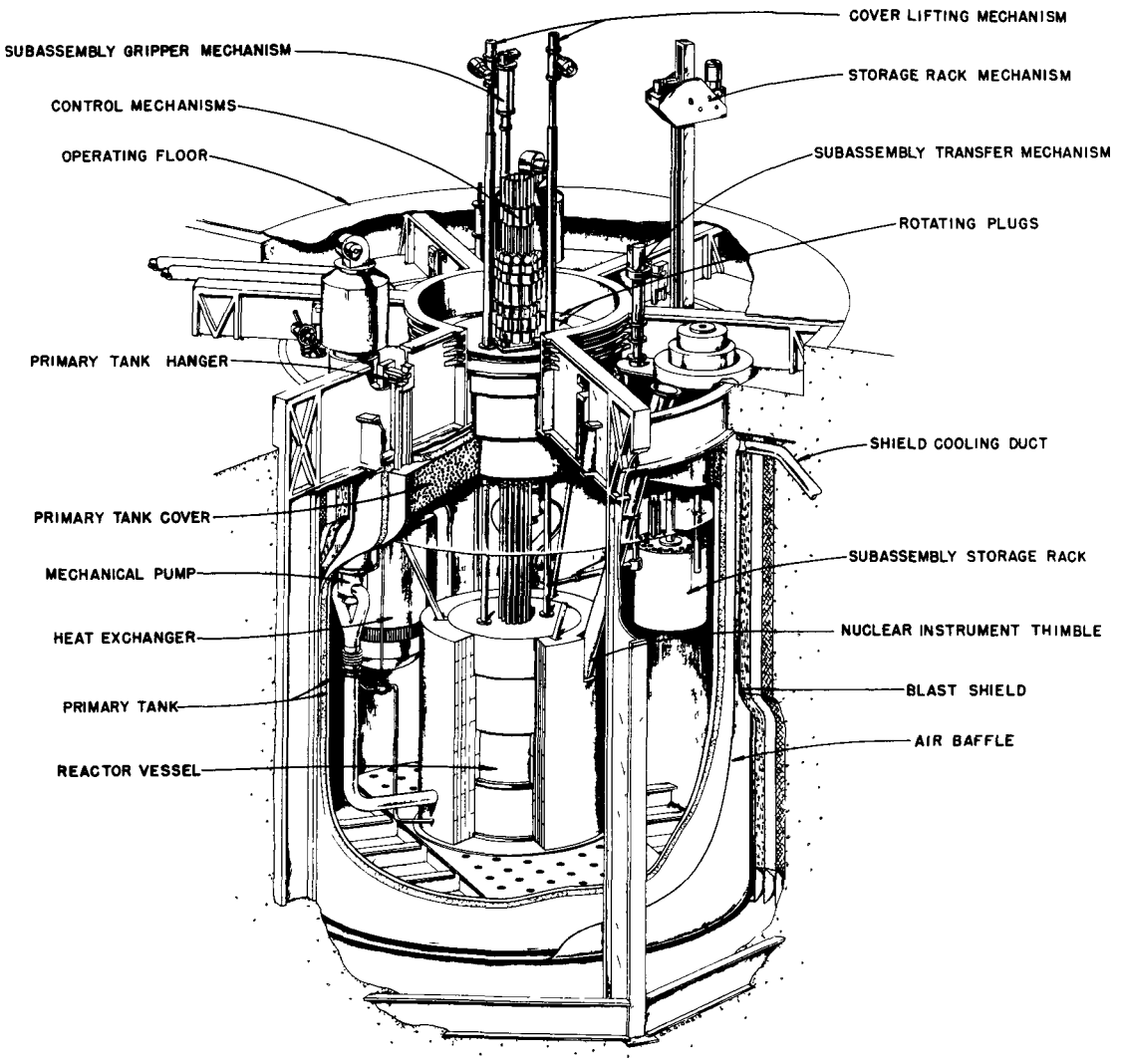

111-6453-B

Fig. 3. EBR-II Primary System

Details of the reactor, the surrounding reactor vessel, and the neutron shield are shown in Figs. 4, 5, and 6. The reactor (core and breeder reflector) is a hexagonal array of subassemblies (Fig. 5). The subassemblies are mechanically designed to prevent inadvertent interchange between enriched and depleted uranium-bearing subassemblies. Each subassembly contains the fissile or fertile material in the form of cylindrical fuel elements bonded with sodium and clad with stainless steel. The fertile material is unalloyed, depleted uranium. The fissile material is contained in uranium-5 w/o fissium fuel alloy. The uranium is 48.4% enriched in U^{235}. Each fuel subassembly contains 91 fuel elements. Each fuel element contains ~67 g of the uranium-5 w/o fissium alloy, for a total of ~2.82 kg of U^{235} per subassembly.

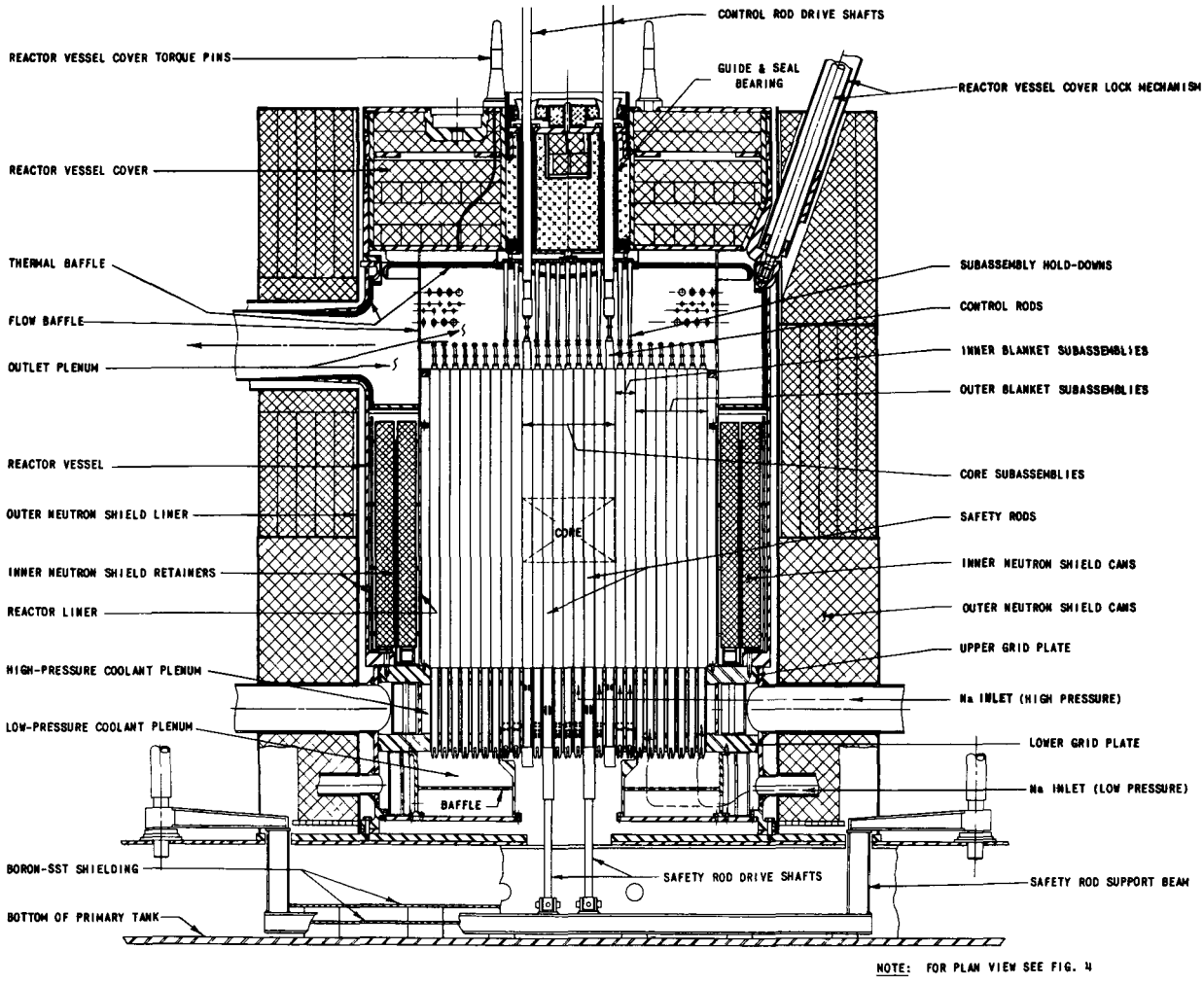

112-496-A

Fig. 4. EBR-II Reactor (vertical section)

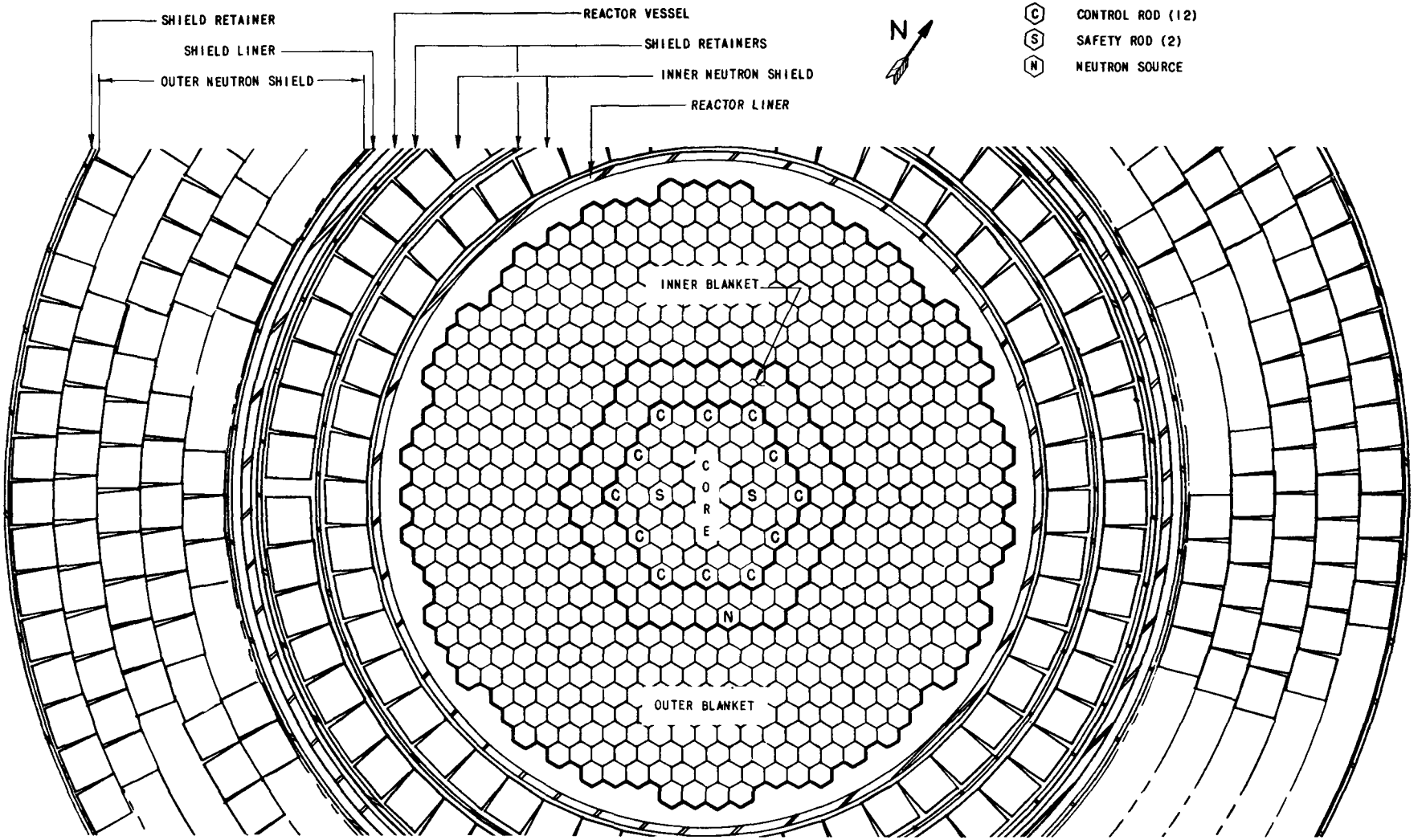

112-789

Fig. 5. EBR-II Reactor (horizontal section)

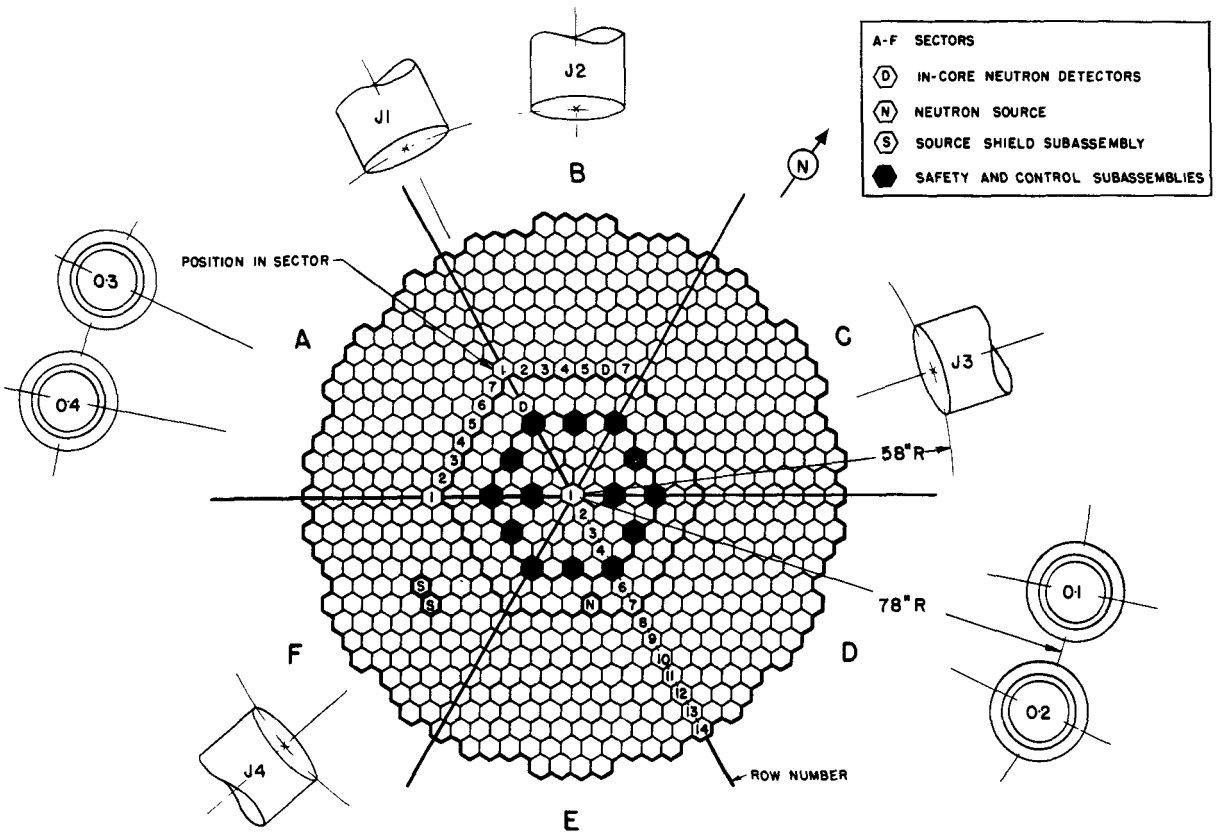

112-411

Fig. 6. Subassembly Loading Diagram

Reactor control is effected by moving fuel into or out of the core from below. There are 12 control subassemblies and two safety subassemblies. Each of these contains 61 of the same fuel elements used in a normal fuel subassembly. Control and safety rod strokes are 14 in., the approximate length of the core. In the most reactive position, the fuel elements in a control rod are at the same elevation as fuel elements in a fuel subassembly. In the least reactive position, the tops of the fuel elements in a control rod are at the same elevation as the bottoms of the fuel elements in a fuel subassembly. The 12 control subassemblies are activated from the top and must be disconnected from their drive mechanisms in their least reactive positions, while fuel is being loaded (Fig. 7). The two safety rods are actuated from below the core (Fig. 4) and are operative while fuel is being loaded. Scram signals actuate these rods in accordance with the mode of operation. During "Reactor Operation," when the reactor is critical, an automatic scram signal will release the 12 control rods. With a pressure assist, the control rods move to their least reactive positions. During "Fuel Handling," when the reactor is expected to be substantially subcritical, an automatic scram signal releases the safety rods. Gravity causes them to move to their least reactive positions below the core. The safety rods may also be manually released during "Reactor Operation."

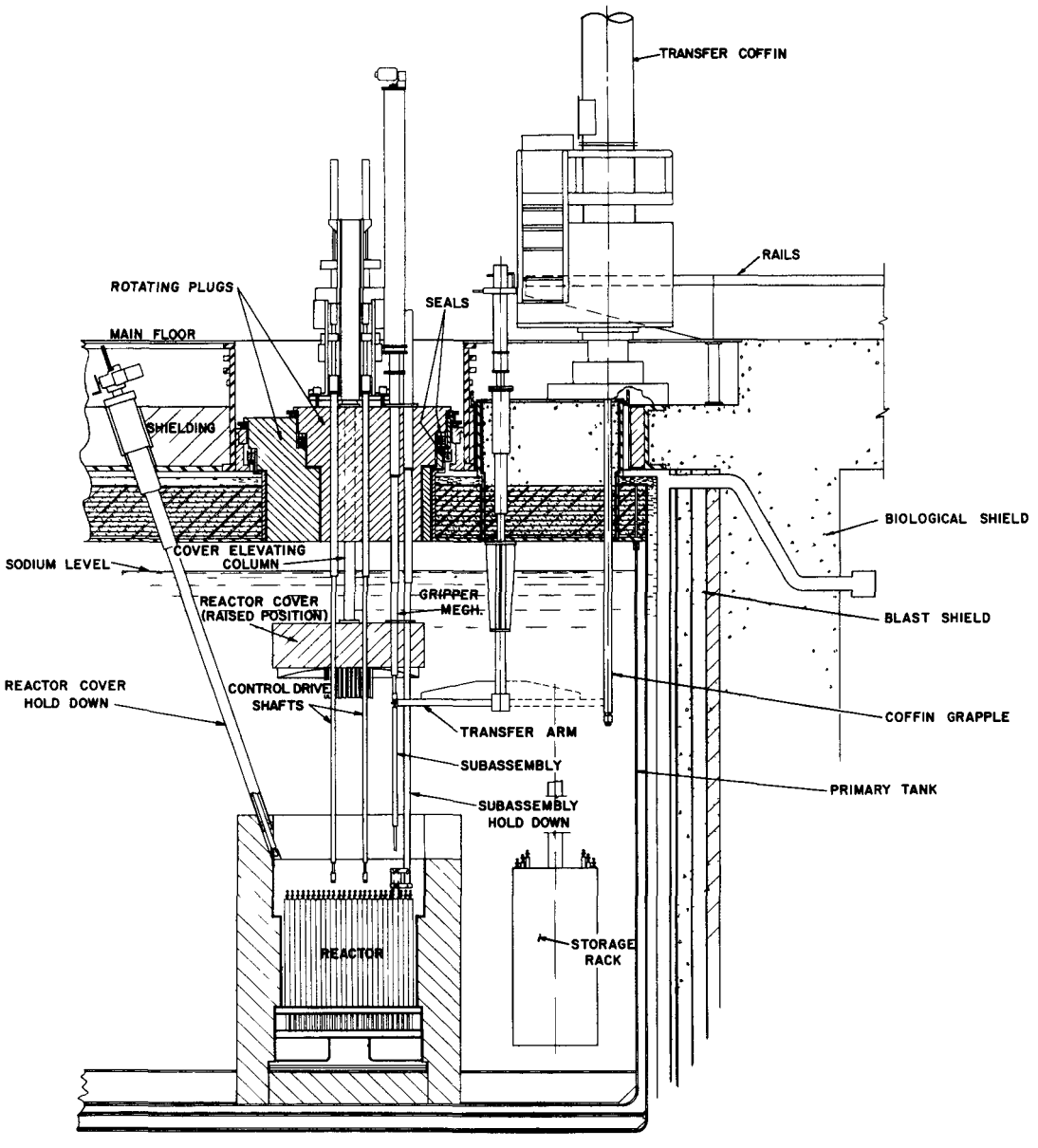

111-6389

Fig. 7. EBR-II Fuel Handling System

The neutron-flux-monitoring equipment (fission counters and ion chambers) are located in eight air-cooled (<45°C) instrument thimbles. Four of these thimbles are embedded in the neutron shield surrounding the reactor vessel (Fig. 8). The other four are located in sodium just outside the neutron shield. The fission counters and ion chambers are located near the central plane of the core for maximum sensitivity, but can be moved vertically inside the thimbles. The neutron shield consists mainly of graphite and borated graphite, canned in stainless steel. Small amounts of sodium pass between the square shield cans. Borated graphite is used only in those shield regions where it does not interfere with instrument response.

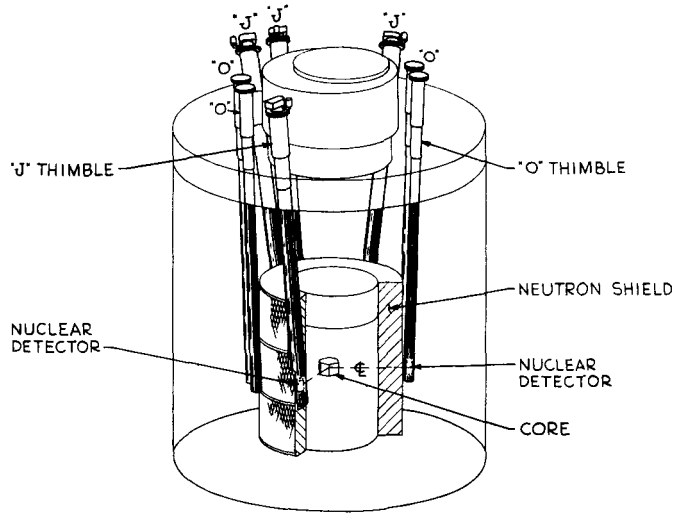

112-435-A

Fig. 8. Nuclear Instrument Thimbles

There is no borated graphite inside the reactor vessel. In the neighborhood of the startup channels (J_1 and J_2 thimbles in Figs. 5 and 8), there is no graphite inside the reactor vessel. There are 11 channels of nuclear instrumentation distributed throughout the eight instrument thimbles. Three log-count data channels are operative from source power to about 0.2 kW. Three log-flux channels and one linear-flux channel are operative from 10 W to full power. Three linear-flux channels are operative from 60 kW to full power. One channel is operative from 6 MW to full power and will be used for automatic control of the reactor at power. Automatic control is not operative until the power level has been manually established.

An antimony-beryllium neutron source subassembly (Fig. 6) will be permanently located in the radial blanket of the reactor. The antimony-beryllium source may be remotely disassembled by reactor fuel-handling equipment. The active antimony rod may be placed in a source shield subassembly located in the outer blanket (Fig. 6).

III. APPROACH TO CRITICAL

A. Neutron Sources

The neutron sources for the Wet Critical Experiments differed slightly from their original design in that the antimony was clad with tantalum instead of stainless steel. Because of the high thermal cross section of tantalum, compared to both stainless steel and antimony (21, 3, and 5 barns, respectively), the irradiation data obtained from the Dry Critical Experiments[1] and the similar ZPR-III Experiments[4] were not directly applicable with respect to the required neutron exposure in the Material Testing Reactor (MTR). Furthermore, changes in the EBR-II reactor schedule for the Approach to Critical made it difficult to optimize MTR irradiations in advance of anticipated needs. As a result, three sources were required to give adequate startup counts. Table I shows the irradiation history of the three sources used, plus two spares and their disposition during the Approach to Critical.

Table I

IRRADIATION HISTORY AND DISPOSITION OF NEUTRON SOURCES USED DURING THE APPROACH TO CRITICAL

Source No.	Irradiation Dates (1963)	Flux (nvt x 10^{20})	Position in EBR-II	Relative Source Strength at Beginning of Critical, 10/30/63
1911	1/21 - 3/11 4/15 - 5/26	3.5 2.9	8-E-2	2.05
1912	7/29 - 8/19 4/15 - 5/26	1.1 0.39	7-E-3	9.5
1913	7/29 - 8/19	1.1	7-E-5	5.5
1914	7/8 - 7/29	1.2	Not used	4.1
1915	9/10 - 10/21	2.2	Standby	-

The high level of tantalum activity of the sources prevented an accurate determination of the antimony activity. However, from the irradiation history and an estimate of the flux perturbation in the MTR due to the tantalum, the estimated total source strength for the three sources was 670 Curies at the start of the Approach to Critical (October 30, 1963).

Count rates in Channels 1, 2, and 3 were less by about a factor of four than would be expected in comparison with source strength data from the ZPR-III mockup.

B. Startup Instrumentation

The startup instrumentation was the same as that described in the EBR-II Hazards Summary Report Addendum.[5] Three fission chambers (Westinghouse No. WX-4245) were designated as startup Channels 1, 2, and 3. Channels 1 and 2 counters were located in the J-1 thimble, and the Channel 3 counter was located in the J-2 thimble (see Fig. 8 for relative location of these instrument thimbles). No special shielding or moderating material was placed around the counters. In addition to the fission counters, two high-sensitivity BF_3 chambers (four Westinghouse BF_3 Model No. W-6998 in one envelope) were placed in thimbles J-2 and J-3. These channels were designated as Channel G and Channel H, respectively. Their sensitivities were greater than the fission chambers by about a factor of ten. These BF_3 detectors recorded more than adequate count rates during the early incremental loadings but were expected to saturate before reactor criticality was reached. Log Flux Channels 4, 5, and 6 and Linear Flux Channel 7 were also operable, but were not expected to give significant neutron flux information until power of the order of one Watt was reached.

C. Loading to Critical

1. Reactor Condition before the Approach to Critical

The configuration of subassemblies within the reactor before the Approach to Critical is given in Fig. 9. The two safety rods and 12 control rods containing 26.5 kg of U^{235} were loaded. The three sources were located as shown in Table I and Fig. 9. The outer blanket (rows 8-16), except for three source shield thimbles, was loaded with standard, outer blanket, depleted uranium subassemblies. The inner blanket (rows 6 and 7) contained standard depleted uranium subassemblies, except at the designated source positions. The core section of the reactor grid (rows 1-5) was loaded with filter subassemblies in rows 1 and 2, steel dummy subassemblies in row 3, steel dummy and natural uranium subassemblies in row 4, and natural uranium subassemblies in row 5.

Just before the first enriched uranium core subassemblies were loaded, the sources were removed and count rates obtained on Channels 1, 2, 3, G, and H to determine the true background (non-neutron) counting rates. The background data, along with the initial count-rate data, are presented in Table II.

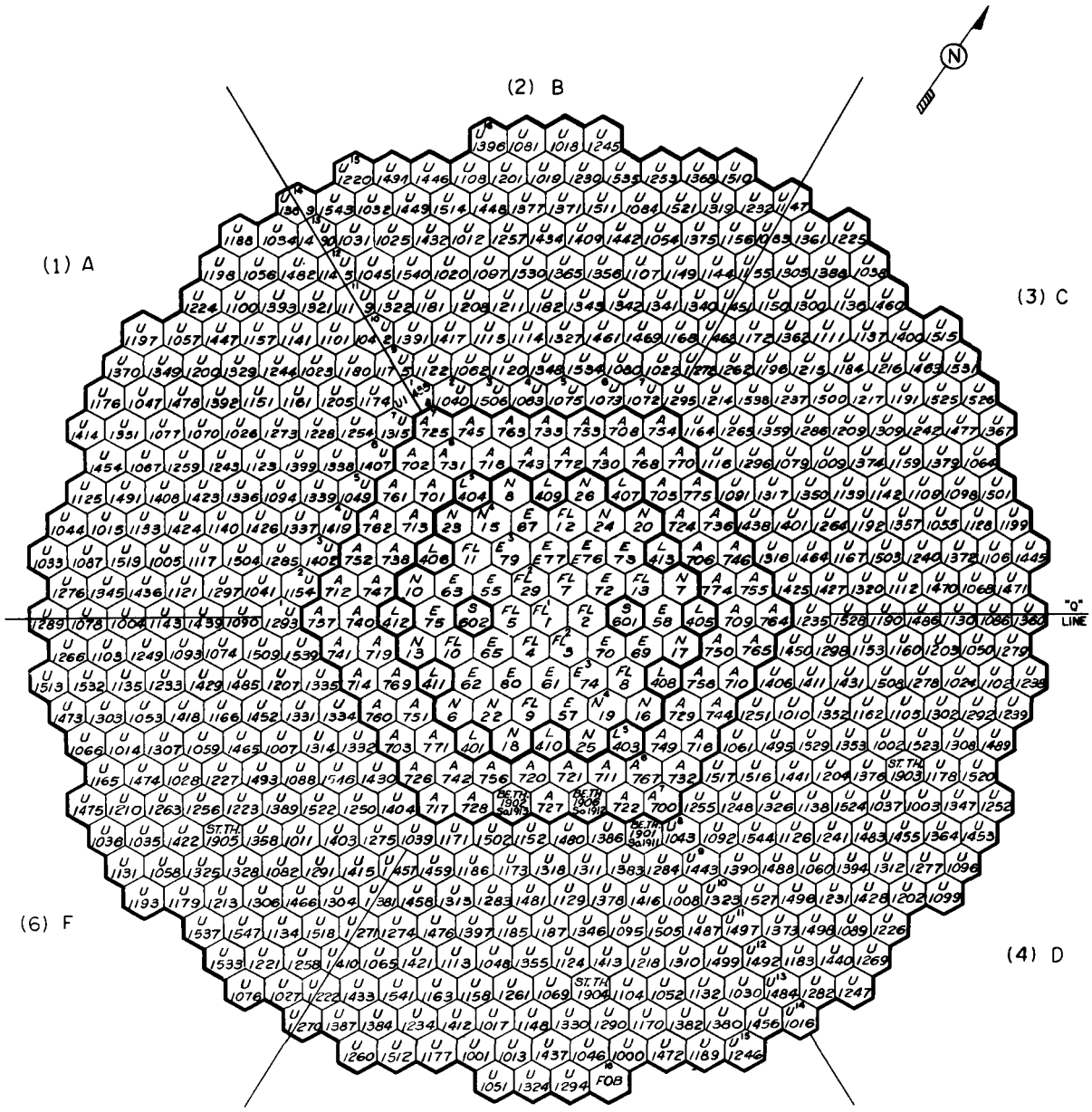

SUBASSEMBLY DESIGNATION	SYM	COLOR CODE
1 – NATURAL "U" CORE	N	BLUE
2 – ENRICHED "U" CORE	C	
3 – CORE DUMMIES (STEEL)	E	BLUE
4 – CONTROL ROD	L	
5 – SPECIAL BORON CONTROL ROD	T	
6 – CONTROL AND SAFETY DUMMIES	D	
7 – SAFETY ROD	S	

SUBASSEMBLY DESIGNATION	SYM	COLOR CODE
8 – SOURCE	SO	
9 – ENRICHED "U" INNER BLANKET	B or D	RED
10 – DEPLETED INNER BLANKET	A	BLUE
11 – INNER BLANKET PLUGGED DUMMY	P	
12 – DEPLETED OUTER BLANKET	U	
13 – STEEL FIXED OUTER BLANKET	FOB	
14 – FILTER SUBASSEMBLIES	FILTER	

ID-103-E5565

Fig. 9. Reactor Configuration before Loading of Fuel Subassemblies

Table II

BACKGROUND AND INITIAL COUNT RATES

Channel	1	2	3	G	H
Background Counts (counts/min)	3	3	5	82	112
Initial Counts* (counts/min)	57	54	60	787	775

* These were obtained at 2300 hours, October 29, 1963, with the three sources in position, 12 control rods "down," and two safety rods in "up" position.

2. Loading of Fuel

The Approach to Critical began on October 30, 1963, with an initial incremental loading of 17 core subassemblies (approximately 2.82 kg of U^{235} per subassembly). Counts on Channels 1, 2, 3, G, and H were taken with the safety rods "up," the reactor cover "down," and the control rods in both "up" and "down" positions. The Approach to Critical proceeded with increments of 6, 6, 6, 6, 5, 4, 3, and 3 core subassemblies per increment, for a total of 56 subassemblies in addition to the two safety rods and 12 control rods. The loading data are presented in Table III, and the corresponding response data from the five counting channels are shown in Table IV.

Table III

LOADING DATA

Loading No.	SA* Added/Loading	Total No. of SA*	kg of U^{235}
1	14	14	26.504
2	17	31	74.277
3	6	37	91.088
4	6	43	108.044
5	6	49	124.956
6	6	55	141.927
7	5	60	155.986
8	4	64	167.291
9	3	67	175.791
10	3	70	184.292

*SA is the total number of fuel subassemblies, including safety rods and control rods.

Table IV

COUNT RATE DATA FOR THE APPROACH TO WET CRITICAL, EBR-II

Loading No.	Channel No. 1		Channel No. 2		Channel No. 3		Channel G		Channel H	
	Control Rods Down (c/m)	Control Rods Up (c/m)	Control Rods Down (c/m)	Control Rods Up (c/m)	Control Rods Down (c/m)	Control Rods Up (c/m)	Control Rods Down (c/m)	Control Rods Up (c/m)	Control Rods Down (c/m)	Control Rods Up (c/m)
1	54	108	51	102	55	113	705	1,710	663	1,676
2	200	280	195	270	213	302	2,581	3,921	2,224	3,422
3	293	417	271	388	306	440	3,659	5,401	3,080	4,591
4	418	637	400	608	447	669	5,114	7,882	4,069	6,291
5	700	1,154	658	1,085	740	1,198	8,079	13,532	6,321	10,286
6	1,199	2,261	1,158	2,162	1,262	2,395	12,797	23,730	10,273	18,706
7	1,861	4,726	1,804	4,523	1,968	4,984	17,457	43,953	14,963	34,951
8	2,768	10,613	2,747	10,527	2,971	11,333		121,628	21,341	66,574
9	3,859	29,593	3,708	28,254	3,957	30,420	41,100	326,695	27,307	111,878
10	5,159		4,947		5,284		57,072		37,732	
Following Control Rods Inserted										
2, 6		6,470		6,294		6,686				
2, 6, 10, 4		8,949		8,626		9,168				
2, 6, 10, 4, 8, 12		13,638		13,340		14,215				
2, 6, 10, 4, 8, 12, 1		17,477		16,885		18,004				
2, 6, 10, 4, 8, 12, 1, 5		23,912		23,182		24,681				
2, 6, 10, 4, 8, 12, 1, 5, 9		37,779		36,586		38,875				

Note: All count rates corrected for background and source decay; c/m = counts/minute.

Reactor critical with nine rods inserted and rod No. 7 at 8.8 in.

In addition to the counts obtained after each loading, counts were also obtained with the reactor cover "up" after the addition of each individual core subassembly. The latter data gave a continuous minimum estimate in terms of how many subassemblies subcritical the reactor was during the loading operation.

Figure 10 shows the numerical loading sequence during the Approach to Critical. The reactor configuration was kept as symmetrical as possible and similar to the loading sequence that was followed during the EBR-II Dry Critical Experiments. Table V is a tabulation of the loading sequence of core subassemblies giving data on each subassembly with respect to serial number, reactor grid position, and isotopic constituent weights.

After each set of counts was obtained, the appropriate correction for background and source decay (half-life of Sb^{124} was taken as 60 days) was applied. The inverse count rate (min/count) was plotted as a function of loaded core subassemblies. Figures 11-15 show these data for each of the five counting channels. Channel G developed amplifier trouble after the eighth loading, and the data were renormalized.

Channel H developed noise after the ninth loading. Since there were adequate counts on Channels 1, 2, and 3, Channel H was not used again.

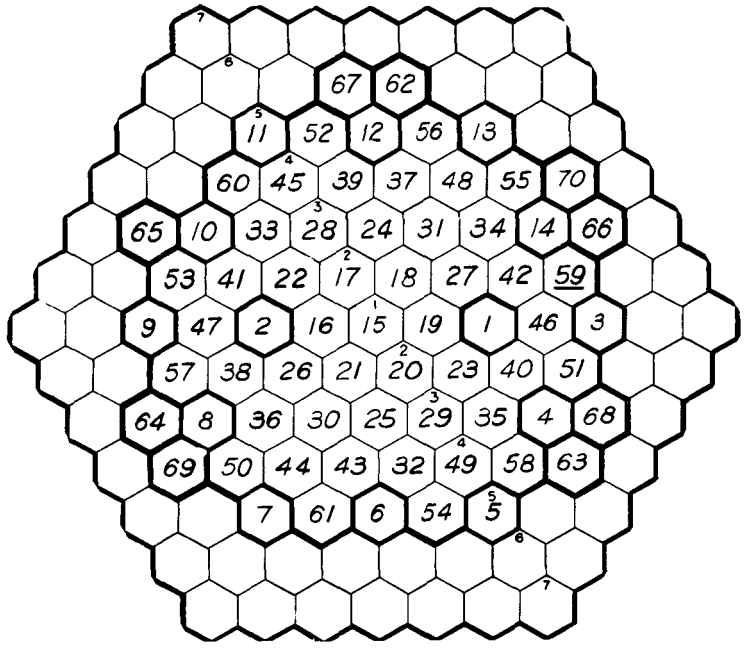

ID-103-E5567

Fig. 10. Diagram of Sequential Loading of Reactor

Table V

LOADING SEQUENCE OF CORE SUBASSEMBLIES

Loading No	Sequence No	Subassembly No	Position	Isotopic Analysis U^{235} (g)	Isotopic Analysis U^{238} (g)
1	1	S 601	3-D-1	1889 90	2037 30
	2	S 602	3-A-1	1883 40	2030 00
	3	L 405	5-D-1	1899 30	2046 50
	4	L 408	5-D-3	1894 30	2041 60
	5	L 403	5-E-1	1899 60	2046 90
	6	L 410	5-E-3	1898 30	2046 10
	7	L 401	5-F-1	1899 50	2046 90
	8	L 411	5-F-3	1888 40	2035 30
	9	L 412	5-A-1	1894 80	2043 30
	10	L 406	5-A-3	1899 60	2046 90
	11	L 404	5-B-1	1899 60	2046 90
	12	L 409	5-B-3	1895 70	2043 00
	13	L 407	5-C-1	1864 53	2009 41
	14	L 413	5-C-3	1896 60	2045 10
2	15	C 138	1-A-1	2804 30	3022 20
	16	C 140	2-A-1	2804 40	3022 00
	17	C 100	2-B-1	2802 00	3019 30
	18	C 143	2-C-1	2804 40	3021 90
	19	C 101	2-D-1	2802 00	3019 30
	20	C 145	2-E-1	2804 40	3022 00
	21	C 122	2-F-1	2833 80	3054 50
	22	C 136	3-A-2	2833 80	3053 50
	23	C 135	3-D-2	2834 00	3053 30
	24	C 134	3-B-2	2833 50	3053 20
	25	C 104	3-E-2	2802 10	3019 10
	26	C 102	3-F-2	2802 00	3019 30
	27	C 139	3-C-2	2802 10	3019 10
	28	C 142	3-B-1	2801 90	3019 40
	29	C 137	3-E-1	2801 90	3019 40
	30	C 103	3-F-1	2802 00	3019 30
	31	C 147	3-C-1	2804 40	3022 00
3	32	C 108	4-E-2	2802 00	3019 20
	33	C 109	4-A-3	2802 00	3019 30
	34	C 110	4-C-2	2802 00	3019 20
	35	C 111	4-D-3	2802 00	3019 20
	36	C 112	4-F-2	2802 00	3019 20
	37	C 113	4-B-3	2801 90	3019 40
4	38	C 153	4-F-3	2804 50	3021 90
	39	C 115	4-B-2	2833 80	3053 60
	40	C 114	4-D-2	2815 60	3034 00
	41	C 119	4-A-2	2833 80	3053 50
	42	C 118	4-C-3	2833 90	3053 40
	43	C 117	4-E-3	2833 80	3053 60
5	44	C 105	4-F-1	2801 90	3019 40
	45	C 149	4-B-1	2804 40	3022 00
	46	C 125	4-D-1	2833 80	3053 50
	47	C 126	4-A-1	2833 80	3053 50
	48	C 127	4-C-1	2833 80	3053 50
	49	C 151	4-E-1	2804 60	3021 60
6	50	C 129	5-F-2	2833 90	3043 50
	51	C 131	5-D-2	2833 80	3053 50
	52	C 121	5-B-2	2833 90	3053 40
	53	C 133	5-A-2	2833 80	3053 60
	54	C 106	5-E-2	2801 90	3019 40
	55	C 116	5-C-2	2833 90	3053 50
7	56	C 107	5-B-4	2802 00	3019 30
	57	C 120	5-F-4	2833 80	3053 60
	58	C 146	5-D-4	2804 60	3011 70
	59	C 144	5-C-4	2804 50	3021 90
	60	C 141	5-A-4	2804 60	3021 80
8	61	C 148	5-E-4	2813 30	3031 10
	62	B 300	6-B-4	2833 80	3053 50
	63	B 301	6-D-4	2833 80	3053 50
	64	B 302	6-F-4	2833 80	3053 50
9	65	B 303	6-A-3	2833 90	3053 40
	66	B 304	6-C-4	2833 80	3053 50
	67	B 311	6-B-3	2832 10	3051 70
10	68	B 312	6-D-3	2833 70	3053 70
	69	B 313	6-F-3	2833 50	3053 10
	70	B 314	6-C-3	2833 80	3053 60

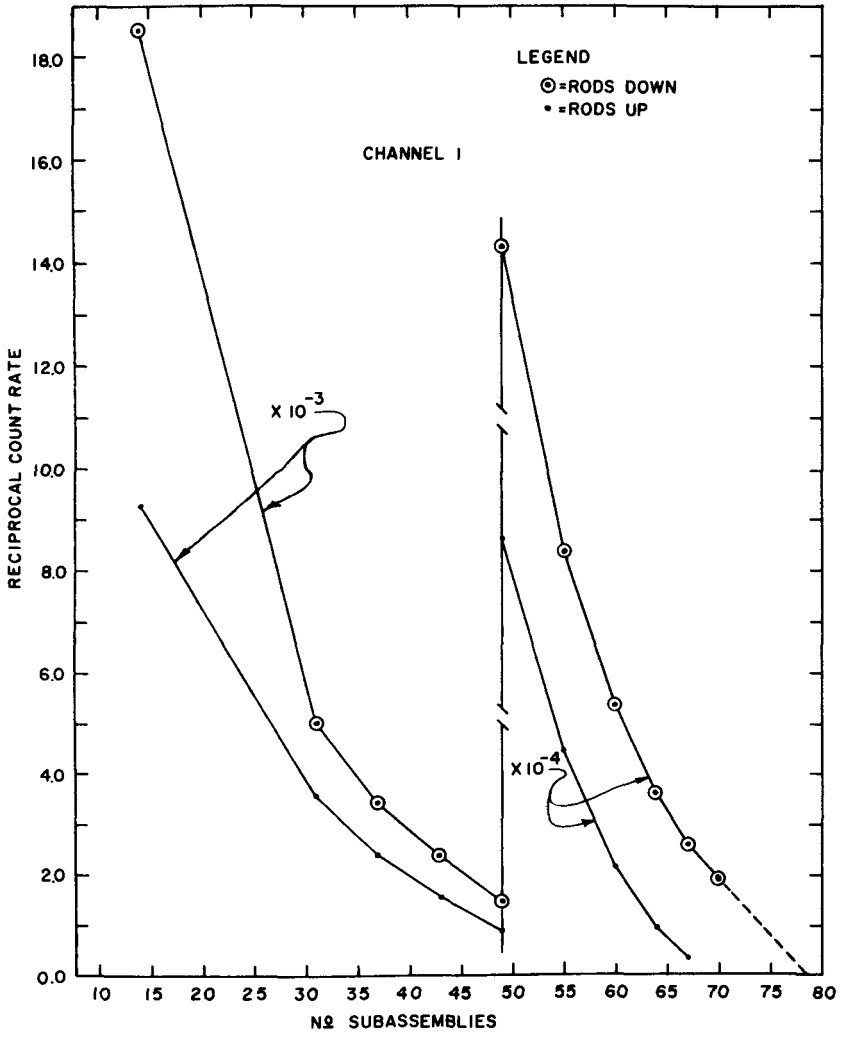

ID-103-E5579

Fig. 11. Inverse Count Rate Versus No. of Subassemblies for Channel 1

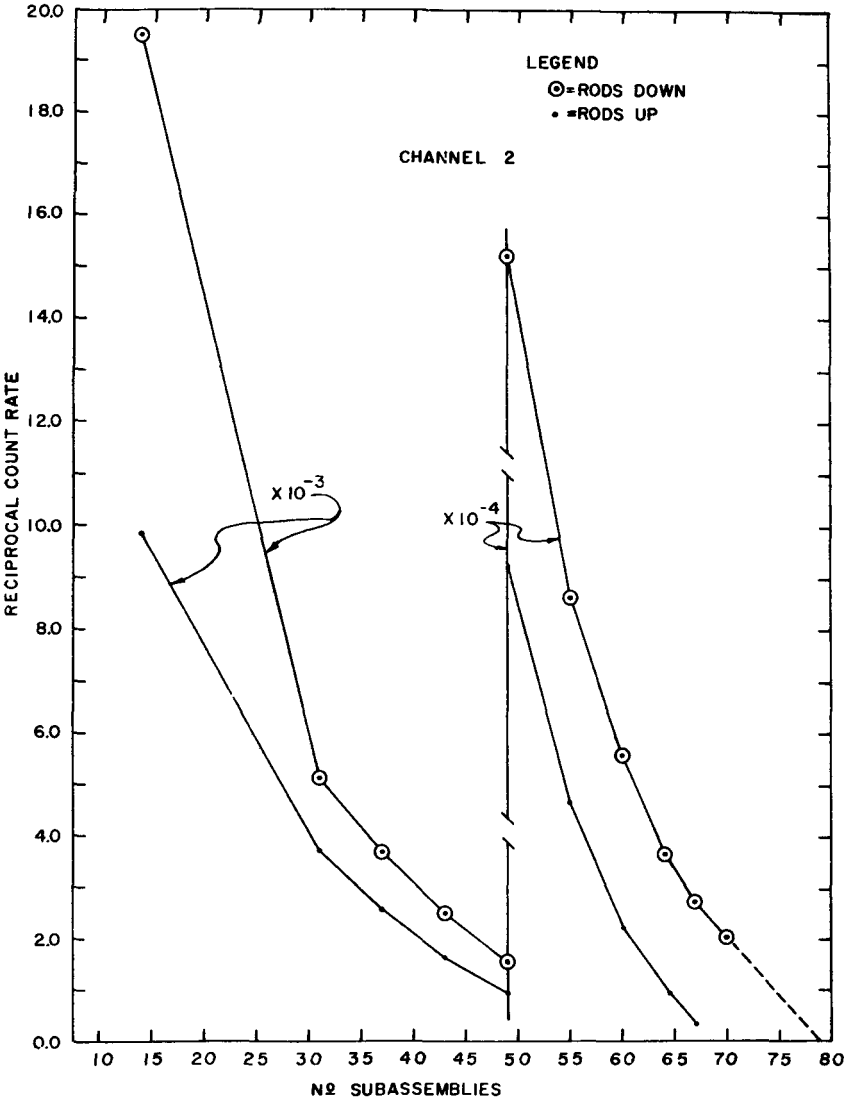

ID-103-E5571

Fig. 12. Inverse Count Rate Versus No. of Subassemblies for Channel 2

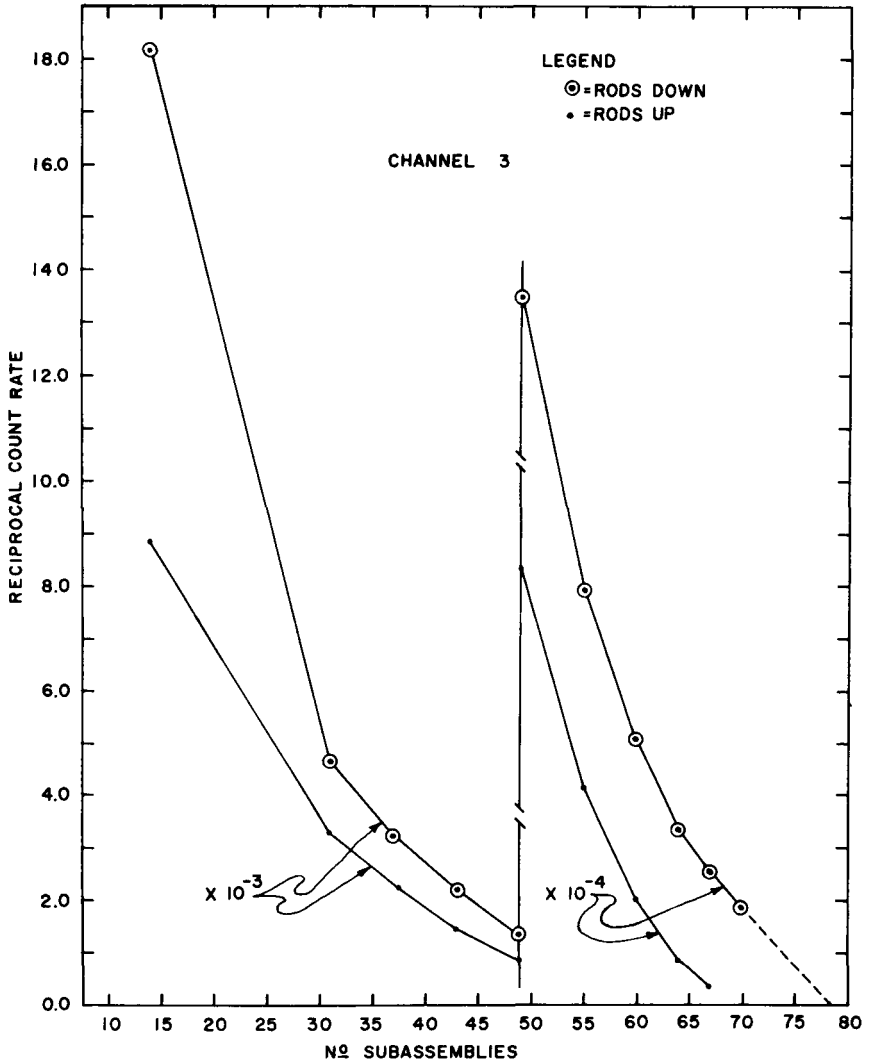

ID-103-E5578

Fig. 13. Inverse Count Rate Versus No. of Subassemblies for Channel 3

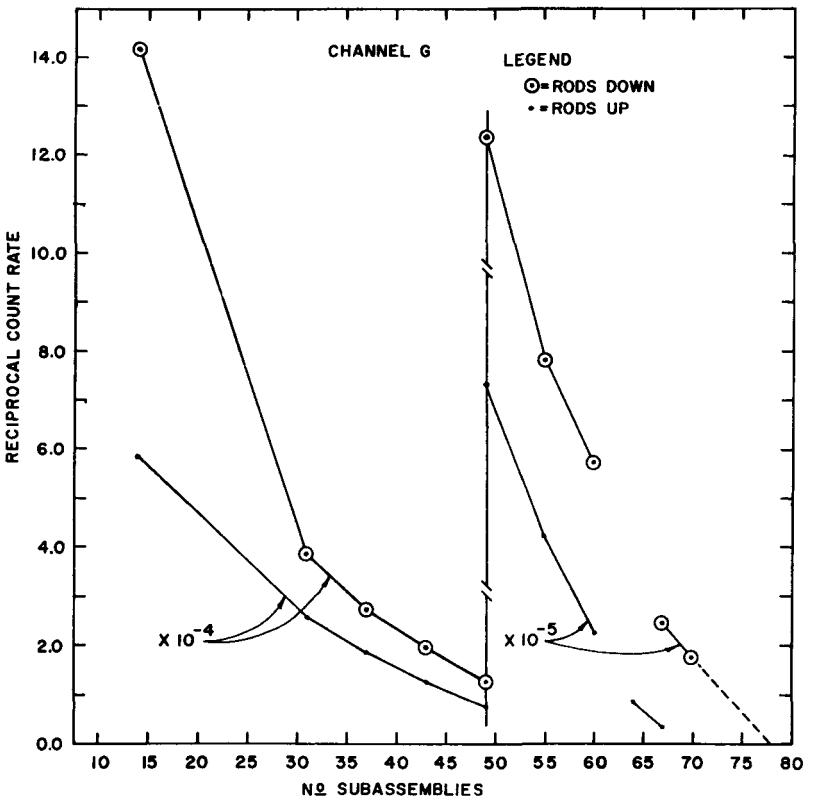

ID-103-E5580

Fig. 14. Inverse Count Rate Versus No. of Subassemblies for Channel G

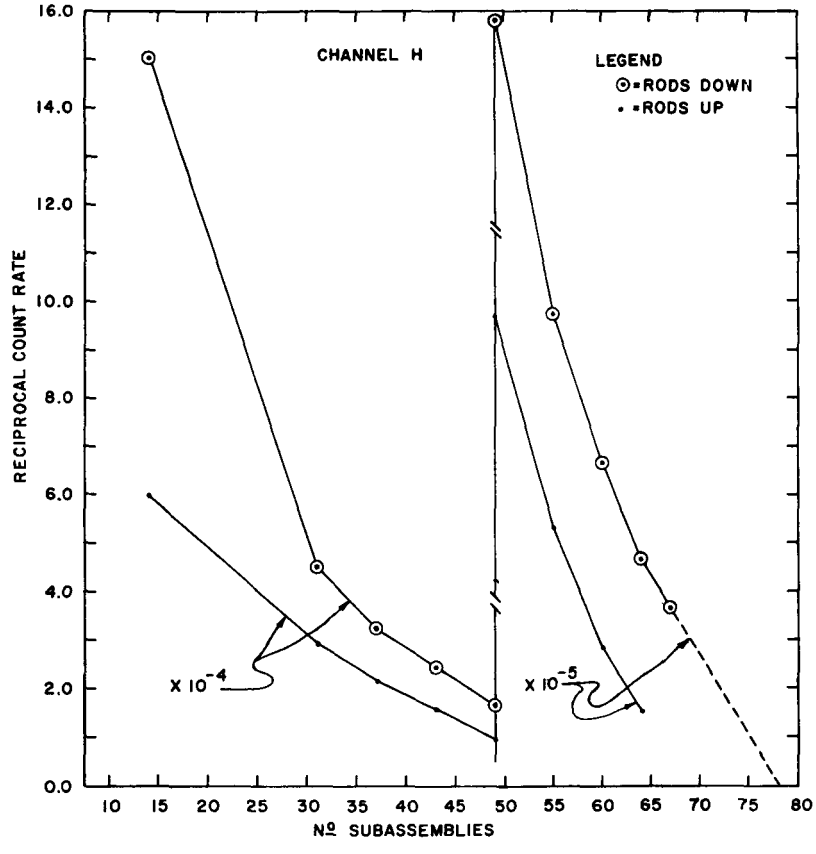

ID-103-E5575

Fig. 15. Inverse Count Rate Versus No. of Subassemblies for Channel H

After each loading was completed, the last two inverse-count-rate data points with the rods "up" were extrapolated to zero, and a conservative estimate of the number of core subassemblies necessary to go critical was determined. The basic criterion for the next loading was that the total number of core subassemblies should not exceed this critical estimate. Obviously, the "final" loading cannot fall within this criterion. Experience obtained from ZPR-III and EBR-I shows that this method of choosing the number of subassemblies for each incremental loading has always proven reliably conservative.

A similar estimate made with the control rods "down" indicated the reactivity worth of the control rods in terms of core subassemblies. Table VI lists the extrapolated number of subassemblies for criticality obtained after each loading for both rods "up" and rods "down" conditions.

Table VI

ESTIMATED NUMBER OF SUBASSEMBLIES REQUIRED TO GO CRITICAL AS A FUNCTION OF THE NUMBER OF SUBASSEMBLIES LOADED

No. SA* Loaded	Channel 1	Channel 2	Channel 3	Channel G	Channel H
		(Rods Up)			
14					
31	41.5	41.4	41.3	44.2	47.5
37	49.1	50.3	51.3	52.5	54.2
43	53.8	53.6	53.3	55.6	59.4
49	56.2	56.7	56.9	58.0	58.0
55	61.2	60.7	60.9	62.8	62.3
60	64.5	64.7	64.6	65.6	65.6
64	67.0	67.6	67.1		68.8
67	68.8	68.3	68.9	68.9	
		(Rods Down)			
14					
31	37.3	37.1	36.9	37.3	38.3
37	49.6	52.3	50.6	51.6	57.6
43	56.3	55.6	55.8	57.8	62.1
49	58.0	58.3	58.2	59.7	61.6
55	63.4	63.0	63.4	65.3	64.2
60	68.9	68.6	58.8	73.2	71.0
64	72.2	71.8	72.6		72.5
67	75.0	75.5	76.1	72.2	
70	78.5	78.9	78.1		

*Core subassemblies (including control and safety rods).

The loading was generally symmetrical, except for the 70th subassembly, which normally would have been placed close to the source in Sector E. Instead, this subassembly was placed in Sector C to avoid the problem associated with an apparent increase in source strength due to the proximity of a fuel subassembly. After 70 subassemblies were loaded, counts were taken after each insertion of two control rods, and an inverse count rate plot was prepared. The relative reactivity worths of control rods located on the corners and flats of the hexagonal core was estimated, and a predicted control rod configuration for criticality was determined. This proved to be correct within a few inches of critical for the final rod insertion.

The reactor diverged on approximately a 60-second period with 11 rods fully inserted at 0245 hours, November 11, 1963. A total of $11\frac{1}{2}$ days elapsed from the beginning of the loading until criticality was achieved.

3. Core Rearrangement and Minimum Critical Mass

After criticality was achieved, the two stronger antimony source rods were removed to the two storage thimbles provided in the outer blanket. The weaker antimony source rod (No. 1911) was moved into the beryllium thimble at grid position 7-E-5 for the remainder of the Wet Critical Experiments. The two empty beryllium thimbles were replaced with standard blanket assemblies. The core fuel loading was then slightly rearranged to give a more symmetrical shape to the core. Figure 16 shows the reactor grid with the final subassembly arrangement, which was then the reference loading for all wet critical measurements.

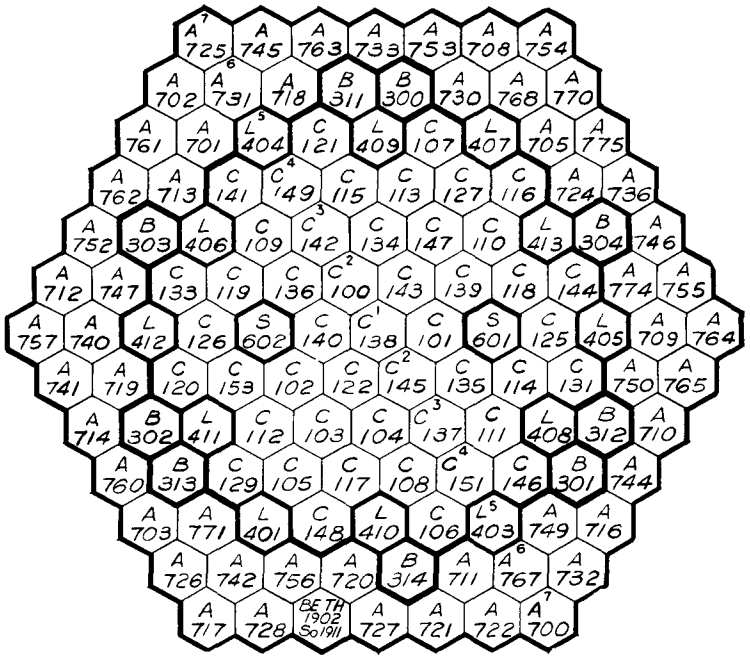

ID-103-E5566

Fig. 16. Reference Loading for Wet Critical Experiments

Subsequent experiments showed this reference loading to have a maximum of 163 inhours (0.39% Δk) excess reactivity at 600°F. This is equivalent to 3.13 kg of U^{235} at the core boundary. (Worth of fuel at boundary is given as 0.35% Δk per subassembly, or 0.125% Δk per kg of U^{235} as mentioned in Section VI below.) Consequently, the minimum wet critical mass is 181.2 kg of U^{235} at 600°F (68.8 core subassemblies, including the safety and control rods). This may be compared to a dry critical mass of 227.9 kg of U^{235}, and the original estimate for the wet critical mass of 172 kg of U^{235}. After the performance of the dry critical experiment, a better estimate of the wet critical mass was established between 176 and 184 kg of U^{235}.

4. Special Irradiation Core Subassemblies

The special irradiation core subassemblies are identical to a standard subassembly, except that the seven central fuel pins have been extensively tested and measured before insertion into a subassembly. These subassemblies are to be used for post-irradiation examination. Originally only seven of these subassemblies were scheduled to be loaded during the Approach to Critical. Twelve were actually loaded into the core position shown in Fig. 17.

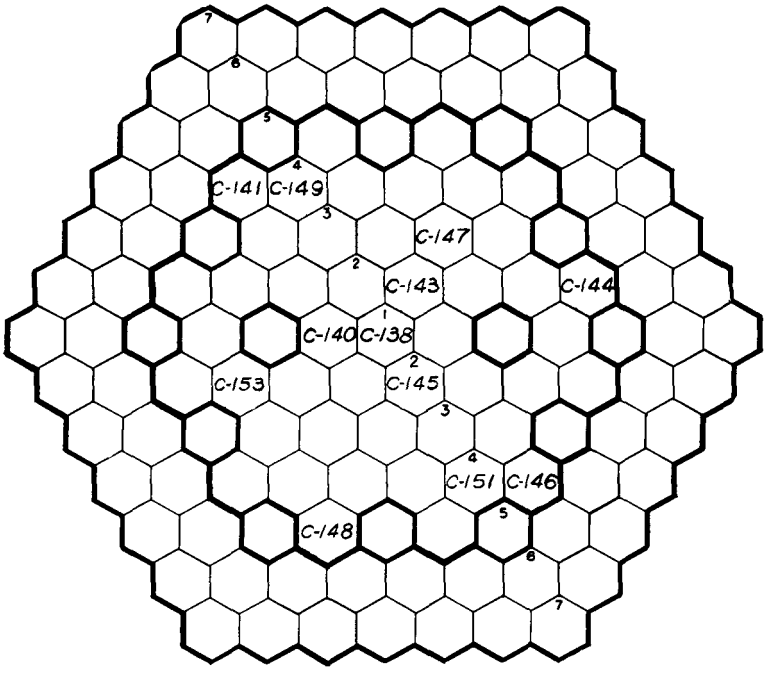

ID-103-E5568

Fig. 17. Position of Irradiation Core Subassemblies

IV. INITIAL POWER CALIBRATION

The two EBR-II source experiments performed on ZPR-III[4] showed that a response of 700 counts/Watt-sec should be expected on Channels 1, 2, and 3. There are many uncertainties in relating this power calibration to the actual conditions in EBR-II. Therefore, the first scheduled experiment was a preliminary power calibration. A special inner blanket subassembly containing two foil holders and one wire holder was inserted into position 6A4. Figure 18 shows the location of the wires and foils within the subassembly and their orientation in the reactor. The U^{235} foils were 1 cm x 1 cm x 1 mil and weighed approximately 54 mg. The U^{238} foils were 1 cm in diameter x 10 mils and weighed approximately 350 mg. The wire holder contained a 30-mil-diam. enriched uranium wire and a 60-mil-diam. depleted uranium wire extending over the length of the core and blanket. The enriched wire was 16.2 w/o U^{235}-aluminum alloy.

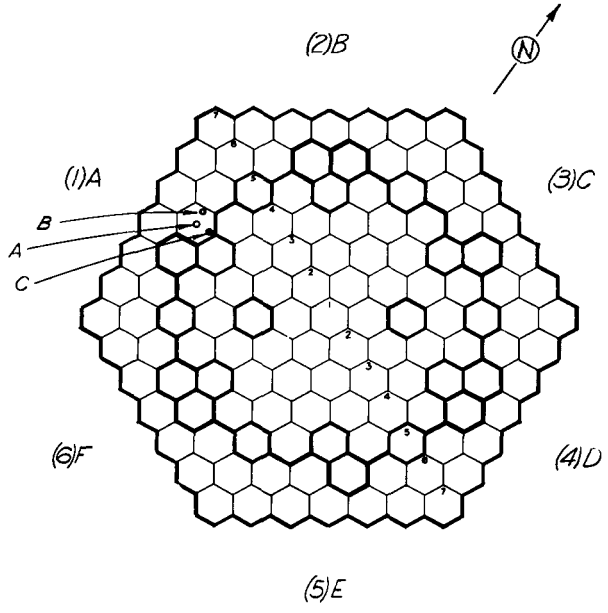

ID-103-E5604

Fig. 18

Location of Power Calibration Foils

The reactor was operated for an estimated kWh, and readings were obtained from all operating channels. (Linear Channel No. 7 was considered the basic power indicator.) After irradiation and subsequent cleaning of the subassembly in the sodium vacuum distillation system, the foils were divided between the Argonne, Illinois, and Idaho Division Laboratories for absolute fission product analysis. The Illinois laboratory measured the fission product Mo^{99} by beta counting, and the Idaho Division measured Mo^{99} by gamma counting. The results are presented in Table VII. A similar power calibration (4 kWh) was made later when the reactor had been cooled to 460°F. This investigation was designed to determine if there was any significant variation in power calibration due to temperature. These data also appear in Table VII and indicate that any variation in instrument response at the two temperatures is less than the accuracy of the measurement.

Table VII

EBR-II POWER CALIBRATION

Temp (°F)	Foil No.*	Foil Weight (mg)	Total Fissions [g (U^2)]	Channel 7 (Amps)	Irradiation Time (sec)	Calculated Reactor Power Level (Watts)**	Calibration (Amps/kW)
600	401 (I)	54.4	5.06×10^{11}				
	402 (C)	54.2	5.03				
	403 (I)	55.0	5.04				
	404 (I)	53.6	4.84				
			Av 5.01×10^{11}	1.3×10^{-8}	7260	650	2.0×10^{-8}
460	415 (I)	54.3	2.33×10^{12}				
	416 (C)	54.0	2.22				
	417 (C)	54.9	2.19				
			Av 2.21×10^{12}				
			Corr. 1.96×10^{12}†	2.6×10^{-9}	14460	1280	2.03×10^{-8}

*The symbols (I) and (C) refer to foils analyzed in Idaho and Argonne, Illinois, respectively.

**Reactor power level was calculated assuming ZPR-III fission distribution, 3.1×10^{10} fissions per Watt-second, and 85% fission in core.

†This is corrected for contribution to the Mo^{99} fission product due to other operating times while fission foils were in the reactor.

From the ZPR-III data and reactor analysis of EBR-II, the ratio of the average fission rate per gram of U^{235} in the core to the fission rate per gram at the foil location was determined to be 0.82. Assuming 3.1×10^{10} fissions per Watt-second, with 85% of the total reactor power produced in the core and 5% of the core power due to U^{238} fission, the number of Watt-seconds to which these foils were exposed may be calculated. These results are given in Table VII. A correction of about 12.5% had to be applied to the data taken at 460°F because of the contribution to the Mo^{99} fission product from other reactor operating times while the special foil subassembly was in the reactor.

The other nuclear instruments were power-calibrated by comparing their outputs to Channel 7. The power calibrations obtained for Channels 1-6 are shown in Table VIII.

Table VIII

CALIBRATION OF NUCLEAR INSTRUMENTS

Channel No.	Calibration
1	390 counts/Watt-sec
2	390 counts/Watt-sec
3	400 counts/Watt-sec
4	6.4×10^{-8} Amp/kW
5	5.3×10^{-8} Amp/kW
6	6.1×10^{-8} Amp/kW
7	2.0×10^{-8} Amp/kW

V. CONTROL ROD CALIBRATION

A. Individual Control Rod Reactivity Worth

Two control rods (No. 7 on a corner and No. 2 on a flat) were period-calibrated from 0 to 14 in. Periods were obtained from both the pulse channels (Nos. 1, 2, and 3) and the linear current channel (No. 7). After each incremental rod insertion, sufficient time was allowed for the stable period to come into equilibrium. Pulse channel results were restricted to data obtained before dead time corrections became significant. Periods obtained from pulse and current channels were in agreement, except in two cases of long periods where the error was less than one and two inhours. Table IX presents the experimental data for the calibration of control rods 7 and 2. Figure 19 shows the corresponding calibration curves.*

Table IX

DATA FOR CONTROL ROD CALIBRATION

Run No.	Control Rod Configurations (in.)			Channels 1, 2, 3 (Av)		Channel 7	
	No. 7	No. 2	No. 11	Period (sec)	Reactivity Worth (Ih)	Period (sec)	Reactivity Worth (Ih)
1	0	14.00	9.26	00	0	0	0
2	3.00	14.00	9.26	127	23.5	134	22.2
3	5.00	14.00	9.26	52	45.0	52.0	45.0
4	5.00	12.50	9.26	72	35.5	69.0	36.8
5	5.00	11.00	9.26	129	23.0	123	23.5
6	5.00	9.11	9.26	00	0	00	0
7	7.00	9.11	9.26	118	25.0	116	25.0
8	8.50	9.11	9.26	59	41.3	58.3	41.5
9	8.50	7.50	9.26	154	19.7	156	19.7
10	8.50	6.25	9.26	00	00	8	0
11	11.00	6.25	9.26	113	25.3	113	25.3
12	12.50	6.25	9.26	71.5	35.7	71.5	35.7
13	14.04	6.25	9.26	59	41.3	58.0	41.5
14	14.04	4.50	9.26	154	19.7	184	17.0
15	14.04	5.00	9.26	113	25.3	123	23.5
16	14.04	3.26	9.26	00	0	00	0
17	14.04	0.0	13.08	00	0	00	0
18	14.04	3.26	13.08	86		88	
19	5.00	9.05	9.26	00	0	00	
20	8.00	9.05	9.26	58		58	

*When the total rod worth was derived, it was assumed that reactivity in inhours is directly proportional to Δk instead of $\Delta k/k$, and that 415 inhours is the equivalent of 1% Δk.

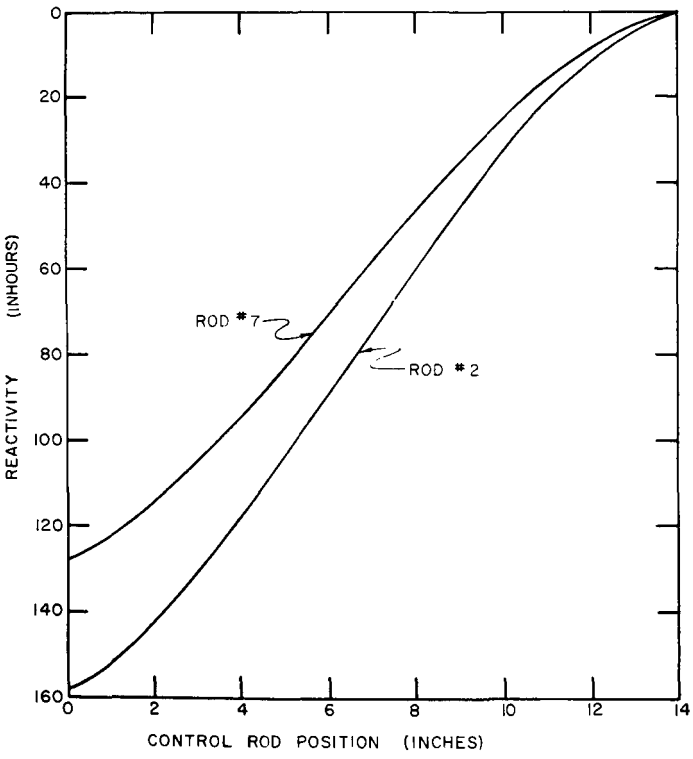

ID-103-E5572

Fig. 19

Calibration Curves for Control Rods No. 2 and No. 7

The individual worths of each of the remaining ten control rods was also determined by intercomparison with control rods 2 and 7. To minimize possible interaction between adjacent control rods, rods 6, 8, and 10 were compared to rod 2; then rods 4 and 12 were compared to control rod 8. Likewise, rods 11, 1, and 3 were compared to rod 7; then rods 5 and 9 were compared to rod 1. The reactivity worths of these ten control rods were also obtained at 7 in. (~50% insertion). Table X shows the results of these comparisons. This table also suggests that the "nuclear center" of the reactor is not at 7 in., but closer to 6.65 in., which is consistent with the nonsymmetric axial reflectors.

Table X

REACTIVITY WORTH OF CONTROL RODS

Control Rod No.	Reactivity Worth at 7 in.*		Total Reactivity Worth	
	(Ih)	(% Δk/k)	(Ih)	(% Δk/k)
1	59	0.142	127	0.306
2	75	0.176	158	0.381
3	61	0.147	130	0.314
4	76	0.183	158	0.381
5	59	0.142	128	0.309
6	75	0.176	157	0.379
7	58	0.140	128	0.309
8	75	0.176	156	0.376
9	59	0.142	128	0.309
10	77	0.186	161	0.388
11	61	0.147	127	0.306
12	75	0.176	157	0.379
Total Worth of Rods			1715	4.13
7 (Boron loaded)**			235	0.566

*~50% inserted

**Special control rod containing 161 g of B^{10} in the form of B_4C was placed in the upper 7 in. of the follower section.

B. Reactivity Worth of Banked Control Rods

Subcritical counting techniques were used to measure the reactivity worth of the 12 control rods banked at several positions. The count rate for the subcritical worth of control rod No. 7 was first established. The reactor was then brought critical with all control rods banked at 10.5 in. Subcritical counts were taken with the control rods banked at 9, 7, 4, and 0 in. (rods "down"). Measurements were also taken with the safety rods "down." From the count rates taken at each position, the corresponding subcriticality can be calculated using the simple formula,

$$\%\Delta k = [CR_7/(CR_T \text{ banked})]\ (0.31\%),$$

where CR_7 is the count rate with control rod No. 7 fully withdrawn from a critical reactor, CR_T banked is the count rate with the rods banked, and 0.31% is the reactivity worth of Control Rod No. 7.

The banked rod data are shown in Fig. 20 as circled data points. For comparison, a calculated curve using the sum of the corresponding,

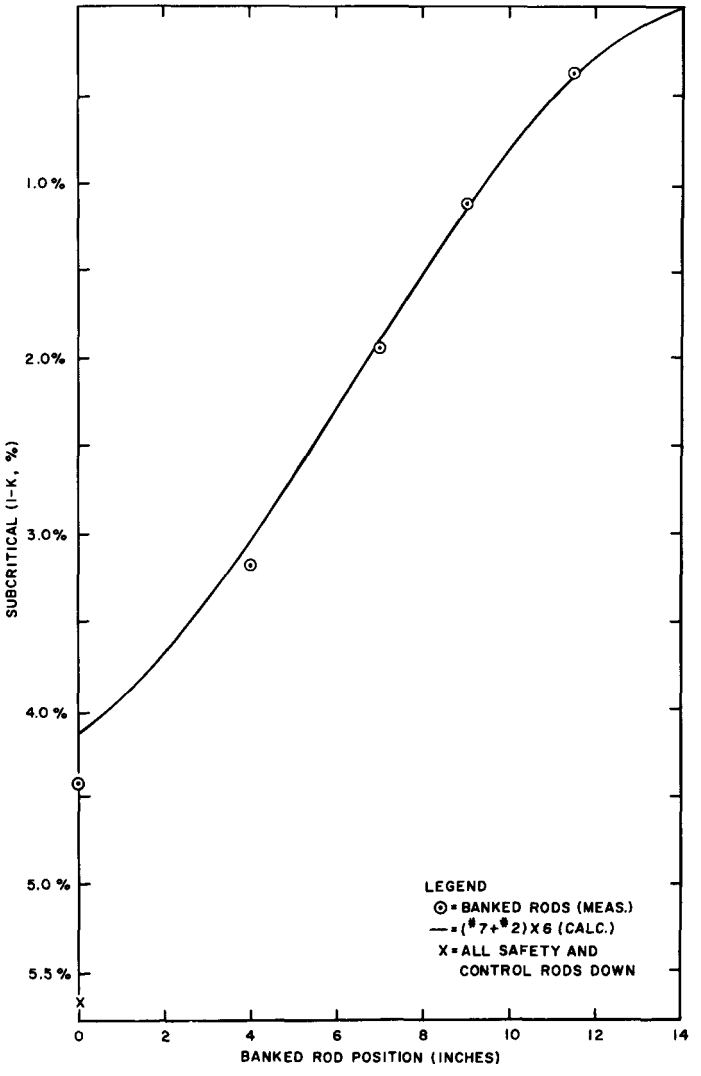

Fig. 20

Worth of Banked Rods

individual reactivity worths of individual rods given in Table XII and on Fig. 19 is shown as a solid line on Fig. 20. The reactivity worth of all control rods "down" is seen to be approximately 4.4% Δk, and with the safety rods "down" approximately 5.6% Δk (an additional 1.2% Δk). Note that the reactivity worth of the banked control rods is more than the sum of the worths of the individual rods. A partial explanation may be that with the rods "down," the reactor is significantly smaller than with the rods "up"; hence, the control rods tend to exhibit greater reactivity worth. Similarly, with the control rods "down," the relative location of the "nuclear center" moves with respect to the monitoring instruments.

The total reactivity worth of the control rods was also measured using the integral count method.[6] This method was used at EBR-I for measuring the reactivity worth of the depleted uranium cup.

With this method, $\Delta k/(1 - \Delta k)$ can be obtained from the following formula:

$$\Delta k/(1 - \Delta k) = \frac{r}{r_0} \sum_{i}^{6} \frac{\beta_1}{\lambda_1},$$

where

r_0 = counts per second at some specific power level,

r = integrated counts obtained after rods are dropped,

β_i = delayed neutron fraction (effective),

λ_i = decay constant for each delayed neutron group,

and

$$\sum_{i}^{6} \frac{\beta_i}{\lambda_i} = 0.0914.$$

In these measurements, the ratio of initial count rate to the integrated counts (corrected for background and timing losses) was measured as 180,000/76,700. The total reactivity worth of the 12 rods from this determination is 4.1% Δk, in fair agreement with the subcritical measurements.

C. Control Rod Shadowing

The effect of one control rod on the reactivity worths of adjacent control rods was measured. The reactor was brought critical on control rod No. 3 with control rod No. 12 at zero in., and control rod No. 7 at 14 in. The subcritical count rate was then obtained with control rod No. 7 at zero in. The positions of control rod No. 7 and No. 11 were interchanged,

and another subcritical count rate was obtained. The difference in count rates shows the effect of a withdrawn rod (No. 12) on the reactivity worth of an adjacent rod (No. 11). The results are presented in Table XI.

Table XI

ROD SHADOWING EFFECT

Rod Positions (in.)			Count Rates (counts/min)	Δk (Ih)
No. 12	No. 7	No. 11		
0	14	14	Critical	0
0	0	14	6924	128
0	14	0	7338	120

Table X indicates that there is an interaction between adjacent rods. This appears to contradict the results of the banked rod experiments, i.e., that all rods "down" hold more reactivity than the sum of the individual, calibrated, control rods. However, banked control rod data also indicate that the banked control rods are worth less than the sum of the individual control rods when the bank is less than 50% removed. The apparent worth of the banked rods tends to increase as the bank is further withdrawn (see Fig. 20).

D. Boron Control Rod Calibration

A special control rod was used during the Dry Critical Experiments to determine the effectiveness of using an absorber in the follower section of a fuel-bearing control rod. This special rod contains approximately 253 g of $B_4^{10}C$ (161 g of B^{10}) in the form of pellets clad with stainless steel. The pellets are mounted in the sodium follower section. The lower extremity is 7 in. above the fuel section and extends for another 7 in. This arrangement is shown in Fig. 21. The special control rod was incrementally calibrated in control rod position No. 7 during the Wet Critical Experiments by comparing it with the previously calibrated control rod No. 2. Since the boron rod held more reactivity than was available as excess reactivity in the reactor, the last 1.1 in. of the rod were subcritically calibrated. The total measured reactivity worth of this control rod was 235 Ih (0.57% Δk), compared with 239 Ih (0.58% Δk) for the subcritical measurements obtained in the Dry Critical Experiments. The calibration curve is shown in Fig. 22. From the ZPR-III mockup of EBR-II, the reactivity worth of this rod was estimated to be 0.55% Δk.

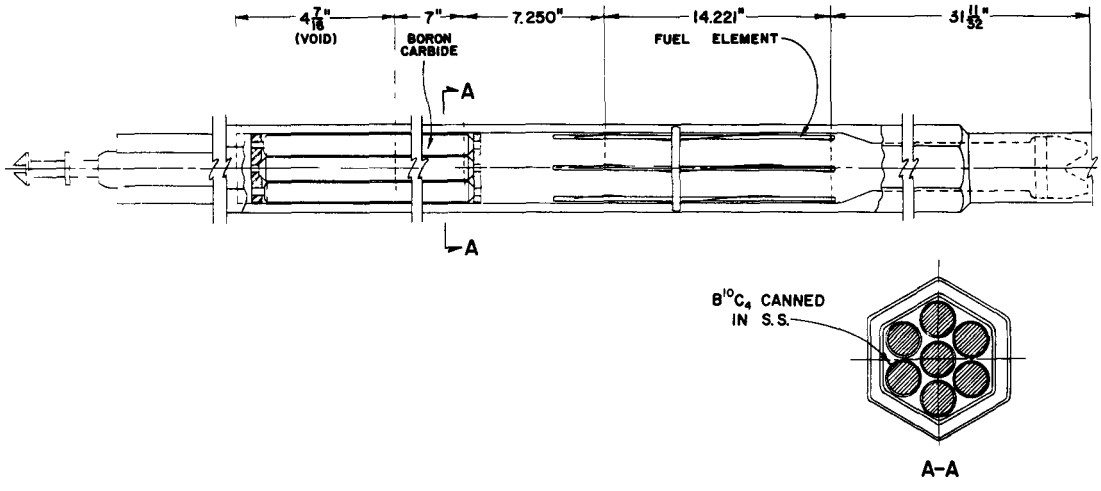

ID-103-E5627

Fig. 21. Special Control Rod Using Boron Carbide

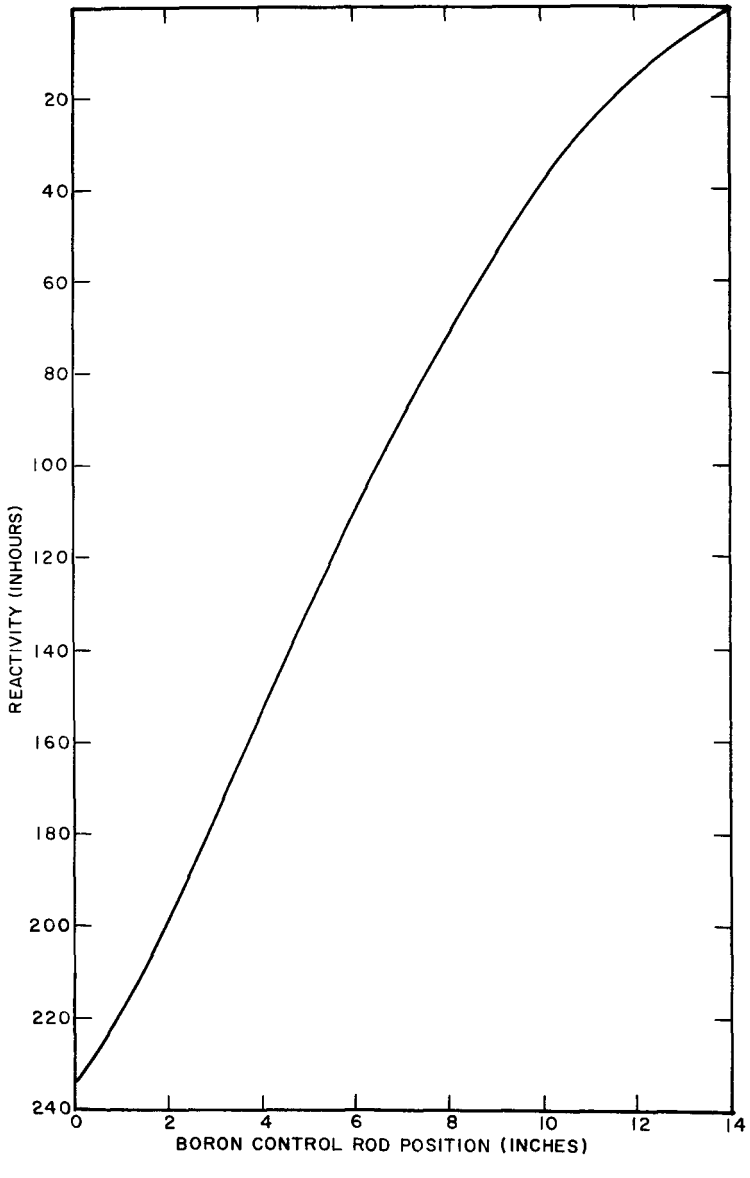

Fig. 22

Calibration Curve for Boron-loaded Control Rod

ID-103-E5574

VI. SUBASSEMBLY SUBSTITUTION

The reactivity worth of a core subassembly was measured as a function of radius. The reactivity worths were determined by replacing core subassemblies containing enriched uranium with natural uranium subassemblies in the core (Rows 1-5), and core type subassemblies containing enriched uranium with standard depleted uranium subassemblies in the inner blanket (Row 6). Such inner blanket measurements will be particularly useful during future power operation for predicting reactivities associated with increasing or decreasing core size. The measurements in the core will serve as a basis for predicting the substitution effects of prototype fuel irradiation subassemblies.

The reactivity worths were measured with respect to the previously calibrated control rods with the reactor either critical or subcritical. All of the subcritical measurements were obtained by observing the count rate with all control rods inserted, and then again with control rod No. 7 withdrawn. The subcriticality is then given by

$$\Delta k = (CR_7)(\Delta k_7)/(CR_{all} - CR_7),$$

Δk = number of inhours subcritical,

where

CR_7 = count rate with control rod No. 7 withdrawn,

CR_{all} = count rate with all control rods inserted,

and

Δk_7 = reactivity worth of control rod No. 7 (128 Ih).

The reference loading had been measured as 163 Ih of excess reactivity before these substitutions. Since some of the substitutions involved larger reactivity increments, subcritical measurements were required to avoid the perturbation of increased reactor core volume. Table XII shows the sequence of loading changes and the measured reactivities.

Figure 23 is a chart of the reactor loading in which the respective reactivity worths in % Δk are inserted into the various reactor positions. The heavy outer line shows the reference loading. Note that the worth of a subassembly is enhanced by the presence of an adjacent fuel subassembly, as shown by the worths of 5D2 versus 5C2 and 6C2 versus 6D2. The data from Table XII are also plotted as a function of radial distance in inches from the reactor center in Fig. 24.

Table XII

SUBASSEMBLY SUBSTITUTION REACTIVITY WORTHS

Run No.	Type of Substitution	Position	Criticality of Configuration (Ih)	Worth of Change	
				(Ih)	(% Δk)
1	Reference loading		163		
2	E → N	5D2	-75	238	0.57
3	N → E	5D2			
	E → N	5C2	-68	231	0.55
4	N → E	5C2			
	E → D	6F4	20	143	0.35
5	D → E	6D1	127	107	0.26
6	E → D	6D1			
	E → E	6D2	161	141	0.34
7	E → D	6D2			
	D → E	6C2	149	129	0.31
8	E → D	6C2			
	D → E	6F4			
	N → E	1,0,0	-337	500	1.20
9	E → N	1,0,0			
	N → E	3B2	-254	417	1.00
10	E → N	3B2			
	N → E	4B2	-164	327	0.79

NOTE: N is a natural subassembly.
D is a depleted subassembly.
E is a fuel subassembly.

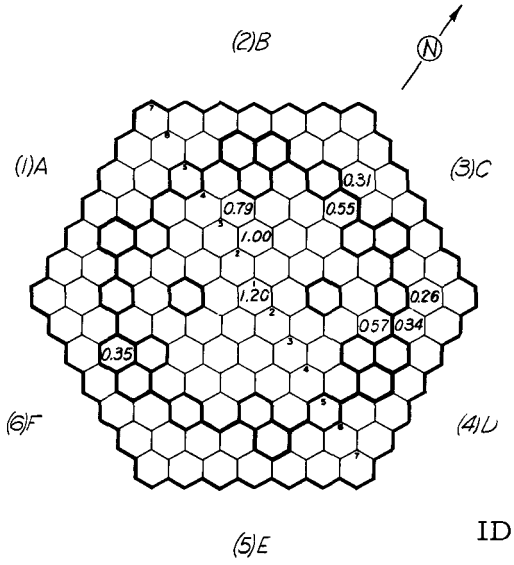

ID-103-E5569

Fig. 23

Chart of Substitution Values in Reactor Core

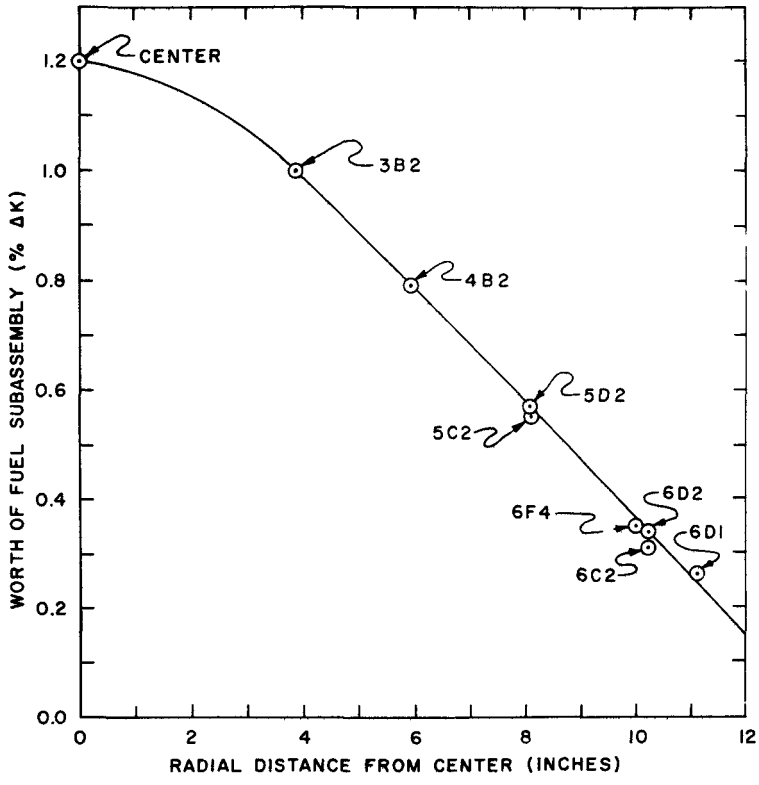

ID-103-E5577

Fig. 24. Fuel Subassembly Worth Versus Radial Position

VII. ISOTHERMAL TEMPERATURE COEFFICIENT OF REACTIVITY

The isothermal temperature coefficient of reactivity was measured by determining the critical control rod position at nominal temperatures of 600, 500, 460, and 550°F ($\Delta T_{max} \approx 140°F$) (see Fig. 25). Temperatures were measured at three locations: the reactor coolant outlet, the high-pressure inlet plenum, and directly above the reactor fuel element subassemblies. Adequate time was allowed at each measured temperature to ensure that the system had come to temperature equilibrium. Since the change between temperature levels was slow, the reactor core and reflector were essentially isothermal at all times. During these tests, the sodium was circulated with the auxiliary electromagnetic (EM) pump at a rate of about 500 gpm.

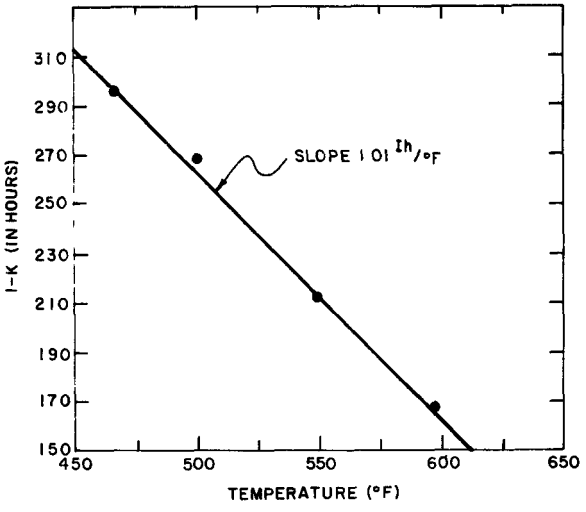

ID-103-E5576

Fig. 25

Isothermal Temperature Curve

Before the above measurements were made, the special foil subassembly was loaded into position 6A4 for a power calibration at the lowest temperature. Critical positions were determined at 50 Watts, and the total, low-power, operating time was minimized to reduce the uncertainties in the power calibration.

The excess reactivity of the reactor as a function of temperature is given in Table XIII for the four temperature levels and the three temperature locations.

The apparent 10°F difference between temperatures from detector No. 1 compared to detectors Nos. 2 and 3 is probably due to thermocouple calibration rather than a real temperature difference. The 24 thermocouples, averaged for the data of detector No. 3, exhibited a spread of about 10°F between individual thermocouples, but these differences also remained constant over the temperature range.

Table XIII

ISOTHERMAL TEMPERATURE COEFFICIENT OF REACTIVITY

Run No.	Date	Time	Temp, °F			Excess Available Reactivity (Ih)
			No. 1	No. 2	No. 3	
1	11/24	1300	597	587.5	588	168
2	11/26	1430	500	492	493.5	266
3	11/27	1440	549	539.5	541	214
4	11/29	0900	465.5	459.5	460	296

Detector No.	Location of Detector	Type	Recorded*
1	High-pressure inlet plenum	Thermocouple	Panel 540, point No. 37
2	Reactor coolant outlet	Resistance thermometer	Measured with a resistance bridge in the cable routing room.
3	Reactor fuel subassemblies	24 individual thermocouples	Average value of data printed on data logging equipment in control room.

*Actual detailed location in Reactor System.

The data from Table XIII were least-squares fitted to a linear function of reactivity versus temperature. An average value of 1.01 ± 0.02 Ih/°F [4.4 x 10^{-5} $(\Delta k/k)/°C$] for the isothermal temperature coefficient of reactivity was obtained from the three sets of data. The reactivity data are plotted in Fig. 13 as a function of detector No. 1 temperatures and were typical of all the measurements.

VIII. IRRADIATED FOIL AND WIRE DATA

The foils and wires used for the power calibration were also analyzed to give the U^{235}/U^{238} fission ratios at the core boundary as well as to provide some indication of the flux gradient through a reflector subassembly. The fission ratios were determined from the absolute number of fissions per gram occurring in the reflector foils and wires. These data are shown in Table XIV. Foils placed at the inner corner of the foil subassembly gave a significant measurement of the flux gradient. This ratio of 1.15 is in good agreement with calculations and the results from the Dry Critical Experiments.(1)

Table XIV

FISSION RATIOS AT CORE BLANKET INTERFACE

Temp (°F)	Material*	Position**	Fission Ratio (U^{238}/U^{235})	C/A U^{235}	C/A U^{238}
600	Foil (I)	A	0.036		
600	Wire (C)	B	0.033		
460	Foil (I)	A	0.037		
460	Foil (C)	A	0.036		
460	Foil (I)	C	0.048		
460	Foil (C)	C	0.046		
				1.15	1.53

*(I) and (C) refer to radiochemical analyses in Idaho and Illinois, respectively.

**See Fig. 18 for appropriate positions of detectors.

IX. REACTIVITY WORTH OF SODIUM

The total reactivity of sodium may be estimated in several ways. The first and most direct method is to look at the difference in the number of subassemblies needed to go critical under "dry" and "wet" critical conditions, and then assign the measured reactivity worth of subassemblies to this difference. This difference, for the two critical conditions, was 16.5 subassemblies applying an average worth of 0.33% Δk for subassembly (see Figs. 23 and 24). The estimated equivalent worth of sodium is 5.5% Δk.

A second method compares the difference in subcriticality of the wet and dry cases for the same number of subassemblies and attributes this difference to the effect of sodium. From the curves for the Approach to Critical, subcritical count rates were obtained with the control rods "up" and "down" at six different loading increments between 55 and 70 subassemblies. The subcriticality of the reactor was then calculated from these data, by using the measured worth of the control rods. An average value of 5.7% Δk was obtained. Both of these methods suffer from attempts to compare two reactor configurations that are not completely comparable. However, these data do agree with the predicted value for the sodium worth of 6.0 $\pm$ 0.5% Δk obtained from measurements in ZPR-III.[2,4]

X. SUMMARY

The EBR-II Wet Critical Experiments were performed over a period of 5-6 weeks. The data obtained confirmed the basic reliability of the predictions made with respect to the fast-reactor physics data for EBR-II.[7] These predictions were the culmination of both calculations and experimental results obtained on ZPR-III and the EBR-II Dry Critical Experiments. Some of the calculated and measured values of EBR-II's nuclear parameters are compared in Table XV.

Table XV

CALCULATED AND MEASURED VALUES OF NUCLEAR PARAMETERS FOR EBR-II

(Nominal Temperature = 315°C, Except Where Noted Otherwise)

	Calculated	ZPR-III Mockup	Dry Critical	Final Prediction	Measured
Critical Mass, kg U^{235}	172	165	228	176-184	181 2
Reactivity Worth, % Δk/k					
Control Rod (Av)	0 45	0 37	0 35	0 34	0 345
Control Rods (12-banked)	-	-	-	-	4 4
Poison ($B_4^{10}C$)[a]	-	0 55	0 58	0 55	0 57
Safety Rods (2)	1 5	1 36	1 0	1 3	1 2
Sodium					
Total	-	6 9	-	6 0 ± 0 5	5 7
Core, (% Δk/k)/kg	0 14	0 116	-	0 116	-
Isothermal Temp Coef , [(Δk/k)/°C] x 10^{-5}					
Structure (Including Fuel)	-1 9	-	-2 6	-2 2 ± 0 4	-
Coolant	-1 7	-	-	-1 8	-
Total	-3 6	-	-	-4 0 ± 0 4	-4 3[b]
Power Calibration, Counts/(Watt)(sec)	-	730	-	500	390
Subassembly Substitution, % Δk/k					
Core Center	1 43[c]	1 53[c]	-	1 26[d]	1 2[d]
Row 5 (Radius = 21 cm)	-	0 77[c]	-	0 64[d]	0 56[d]
Row 6 (Radius = 27 cm)	-	-	0 35[d]	-	0 35[d]

[a]Optional control rod containing 253 g of 87% enriched $B_4^{10}C$ in upper 7 in of control rod follower
[b]Measured at 237-315°C
[c]Enriched subassembly versus sodium
[d]Enriched subassembly versus U^{238} subassembly of identical composition

ACKNOWLEDGMENTS

The execution of these experiments was possible only as the result of the combined efforts of many people in both EBR-II Project and Operation organizations. Their contributions are gratefully acknowledged. Special thanks are given for the help of P. I. Amundson, J. M. Gasidlo, and R. L. McVean of the ZPR-III staff who contributed their time and effort principally during the loading effort. We also express our thanks to E. R. Ebersole (ID) and R. J. Armani (RP) who did the foil analysis.

REFERENCES

1. R. L. McVean, et al., EBR-II Dry Critical Experiments, ANL-6462 (Feb 1962).

2. J. K. Long, et al., Fast Neutron Power Studies with ZPR-III, Proc. of 1958 Geneva Conference. Vol. 12, p. 119 (Paper No. 598).

3. R. Avery, et al., The Physics of Fast Reactors, Geneva Conference Paper No. 259 (1964).

4. W. P. Keeney and J. K. Long, Zero Power Reactor-III, Idaho Division Summary Report, July-September 1960, ANL-6301, p. 45.

5. L. J. Koch, et al., Addendum to Hazards Summary Report, Experimental Breeder Reactor-II (EBR-II), ANL-5719 (Addendum), (June 1962).

6. Idaho Division Summary Report, October 1960 through March 1961, ANL-6392, p. 7.

7. W. B. Loewenstein, The Physics Design of EBR-II, Proc. of IAEA-Sponsored Seminar on the Physics of Fast Reactor, Vol. III, p. 263 (1962).